REPUBLIC OF IRAQ
MINISTRY OF HIGHER EDUACTION &
SCIENTIFIC RESEARCH
AL MUTHANNA UNIVERSITY
COLLEGE OF SCIENCE

A STUDY OF MAGNETIC PROPERTIES FOR A FERRIMAGNETIC BINARY ALLOY WITH DIFFERENT CRYSTAL FIELDS

A THESIS SUBMITTED IN PARTIAL FULFILLMENT OF THE REQUIRMENTS FOR THE DEGREE OF MASTER IN PHYSICS SCIENCES

BY

HASAN FAREED FAWZI

Supervisor

Asst. Prof. Dr. Hadey Kasim Mohamad

2018


بسم الله الرحمن الرحيم
﴿ يَرْفَعِ اللَّهُ الَّذِينَ آمَنُوا مِنْكُمْ وَالَّذِينَ أُوتُوا
الْعِلْمَ دَرَجَاتٍ وَاللَّهُ بِمَا تَعْمَلُونَ خَبِيرٌ ﴾
سورة المجادلة – الآية (11)
صَدَقَ اللهُ العَلِيُّ العَظِيم

Certificate

I certify that this thesis entitled "***A Study of Magnetic Properties for a Ferrimagnetic Binary Alloy with Different Crystal Fields"*** was prepared by ***"Hasan Fareed Fawzi"*** under my supervision at the department of physics, College of science, Al Muthanna University as a part of the requirements of the Master degree of Science in physics.

Asst. Prof. Dr. Hadey K. Mohamad

Supervisor

Date:

Recommendation of the head of physics Department

In view of the available recommendations, I forward this thesis for debate by the examining committee

Asst. Prof. Ali Salman Ali

Head of the department

Date:

ABSTRACT

In this work, the magnetic properties of a mixed spin-3/2 and spin-5/2 Blume-Capel Ising system are investigated for a series of molecular based magnets, which is numerically solved by using the Oguchi approximation (OA) of a simple cubic lattice (sc) and face centered cubic one (fcc), respectively. Oguchi method deals with a single pair of neighboring atoms and assuming that the pair is coupled to the rest of the lattice through an effective field, which is more realistic comparing to the Mean-Field approximation. The magnetic anisotropies have carefully been changed so that one can examine interesting phenomena such as compensation behaviors and free energy of the system, where these phenomena find that the mixed-spin Blume-Capel Ising system considered has one compensation temperature when ($D_B/|J| = -2.8$) with various values of $D_A/|J|$ for a simple cubic lattice (z=6). Whereas the concerned system has three compensation points for a simple cubic lattice in the range of ($-1.99 \leq D_B/|J| \leq -1.85$) and for face centered cubic one (z=12) in the range of ($-5.2 \leq D_B/|J| \leq -4.8$), respectively. The appearance of compensation points has been noticed to be of $D_A/|J|$; however $D_A/|J|$ influences the magnitude of these points in the temperature space. It is worth to note that this phenomenon does not appear in the case of positive values of magnetic anisotropies. It is concluded that the considered system maintains its phase whether the system is in first order or second order phase transition. On the other hand, the obtained results indicate that the considered system has experienced the second order phase transition. A series of behaviors' types has been obtained for both structural lattices, which are Q, P, S, N, L, M, type for (sc) lattice and Q, S, N, R, L, M, type for (fcc) lattice. Besides, it has been studied the contribution of free energy to the thermodynamic phase stability of our system. The free energy as a function of temperature has been established using the partition function Z.

Experimental studies have been performed for compounds with elements contains a spin-3/2 and spin-5/2 such as $Cs_2Mn^{II}[V^{II}(CN)_6]$, $CsMn^{II}[Cr^{III}(CN)_6].H_2O$ and $Mn^{II}[Mn^{IV}(CN)_6].x.H_2O$ which are all crystallized in fcc structure. It remains to mention that the occurrence of a compensation point is of great technological importance since at this particular point a small driven field is required to change the sign of the resultant magnetization; this property is useful in reducing the area of the hysteresis loop (less energy losses) in the ferrimagnetic compounds mentioned earlier.

ACKNOWLEDGMENTS

First, I would like to express my sincere gratitude to my advisor Asst. prof. Dr. Hadey K. Mohamad for the continuous support of my MSc. study and related research, for his patience, motivation, and immense knowledge.

Besides my advisor, I would like to thank the Deanship of Science College in Al Muthanna University especially the Dean and head of Physics department Asst. prof. Ali Salman Ali, who provided me an opportunity to be part of this intellectual society. Besides, one has to thank Dr. Hassan M. Jaber for his efforts and his remarks in this respect. Without their precious support and useful insights, it would not be possible to conduct this research. In addition, I should never forget my colleagues Saja, Hussain, Furqan, and Baida'a who accompanied me during this scientific journey, thank you.

Finally, I must express my very profound gratitude to my parents, my brother and sisters for providing me with indefinite support and continuous encouragement throughout my years of study and through the process of researching and writing this thesis. This accomplishment is dedicated to them, which would not have been successful without them, thank you.

Hasan Fareed

TABLE OF CONTENTS

LIST OF FIGURES

LIST OF TABLES

LIST OF SYMBOLS AND ABBREVIATIONS

Abbreviation	Key
I	Current (A)
m	Magnetic moment (A/m)
A	Area (m^2)
M	Total Magnetization (A/m)
T_C	Curie Temperature (*k*)
B	Magnetic Flux Density (T)
H	Magnetic Field (A/m)
T	Temperature (*k*)
χ	Susceptibility
C	Curie Constant
M_S	Saturation Magnetization (A/m)
M_o	Saturation Magnetization at T=0 (A/m)
T_N	Neél Temperature (*k*)
D	Single-ion anisotropy or Crystal Field (J)
S	Spin Quantum Number
e	Electron Charge (C)
c	Speed of Light in Vacuum (m/s)
ν	Velocity (m/s)
h	Planck Constant (J.s)
H_m	Molecular Field (A/m)
w	Molecular Field Coefficient
N	Number of Atoms
k_B	Boltzmann Constant (J/*k*)
H	Hamiltonian (J)
S_i, S_j	Spin of atom in site *i* and *j*, respectively
h_i, h_j	Effective-Field Parameters (J)

β	Lagrange Multiplier (1/J)
H_{OA}	Hamiltonian in Oguchi Approximation (J)
μ_B	Bohr Magneton (J/T)
m_A, m_B	Sublattice magnetizations of A and B sites, respectively (A/m)
F	Free Energy (J)
Z	Partition function
J	Exchange interaction (J)
D_A, D_B	Single-ion Anisotropy on A and B sites, respectively (J)
T_K	Compensation Point (k)
z	Number of Nearest Neighbors
g	Landé g-factor
TM	Transition Metals
RE	Rare Earth Metals
MFA	Mean-Field Approximation
OA	Oguchi Approximation
fcc	Face-Centered Cubic
bcc	Body-Centered Cubic
sc	Simple Cubic
BC	Blume-Capel Model

CHAPTER ONE

General Introduction

1.1 Introduction

The magnetic material, longest known to man, is lodestone or magnetite, which has, basically, the chemical constitution Fe_3O_4 or $FeO.Fe_2O_3$, i. e. ferrite. It was known to the ancients that this mysterious substance had attracted other bodies of same nature [1].

All materials are magnetic, this means that every material responds to an external magnetic field in a specific manner. The origin of magnetism lies in a very basic principle, i.e. a moving charge (namely, current) produces a magnetic field. Thus, it has been found that a current carrying coil behaves similar to a bar magnet and produces a magnetic moment (m), which is found to be equal to the product of the current (I) and the area (A) of the loop [2].

$$m = IA \tag{1.1}$$

Magnetic solids have numerous and important technological applications: the researchers have found a wide use of information storage devices, microwave communication systems, electric power transformers, dynamos and high-fidelity speakers. By far the largest application of magnetic materials is in information storage media, and the annual sales of computer diskettes, compact disks, optical disks, recording tape, and related items exceed those of the celebrated semiconductor industry. The demand for higher bit-density information storage media and the emergences of new technologies such as magneto-optic devices makes it crucial to expand the search for entirely new classes of magnetic materials [3].

The magnetism originates from the atomic subshells of a cloud of polarized electrons in a number of atoms, then it results from the individual electrons in the energy levels and the electronic charge will flow. In the case of atoms, the total angular momentum for an electronic cloud will originate a magnetic field perpendicular to the spin of the electrons [4].

In the presence of external magnetic field, the magnetic moments within a material tend to become aligned with the field and reinforced it by virtue of their magnetic fields. As a result of this alignment, a new quantity will appear namely the magnetization (M) of the solids [5]. There are types of magnetic materials that have a non-zero net magnetization in the absence of magnetic field, such as ferromagnetic and ferrimagnetic materials i. e. the magnetic moments are already aligned. This unique property depends on the temperature; with increasing temperature, the net magnetization will decrease until it reaches zero at a certain point called the Curie temperature T_C [6].

1.2 Magnetic Domains

Weiss made one of the most important advances in understanding ferromagnetism in two papers published in 1906 and 1907, respectively [7]. In these papers, Wiess suggested the existence of magnetic domains in ferromagnets. These domains have a large number of atomic moments that are aligned together, typically 10^{12} to 10^{15}, so that the magnetization inside a domain has a non-zero value at the absence of any external field. However, the direction of alignment varies from domain to domain in a random manner, although certain crystallographic axes are preferred by the magnetic moments, which will become parallel with one of these equivalent magnetic easy axes [8].

These regions are separated by thin walls called the domain walls, inside these walls the magnetization must change direction from one easy crystallographic direction to another. This change in direction does not occur abruptly, but in such a way that it changes gradually over many atoms inside the walls which means that the walls in general have a non-zero width about (10-100) nm and a definite structure. These walls are often called Bloch walls since F. Bloch made the first theoretical examination of domain walls in 1932 [9]. Figure 1.1 shows how the magnetic moments change their direction gradually within the domain wall.

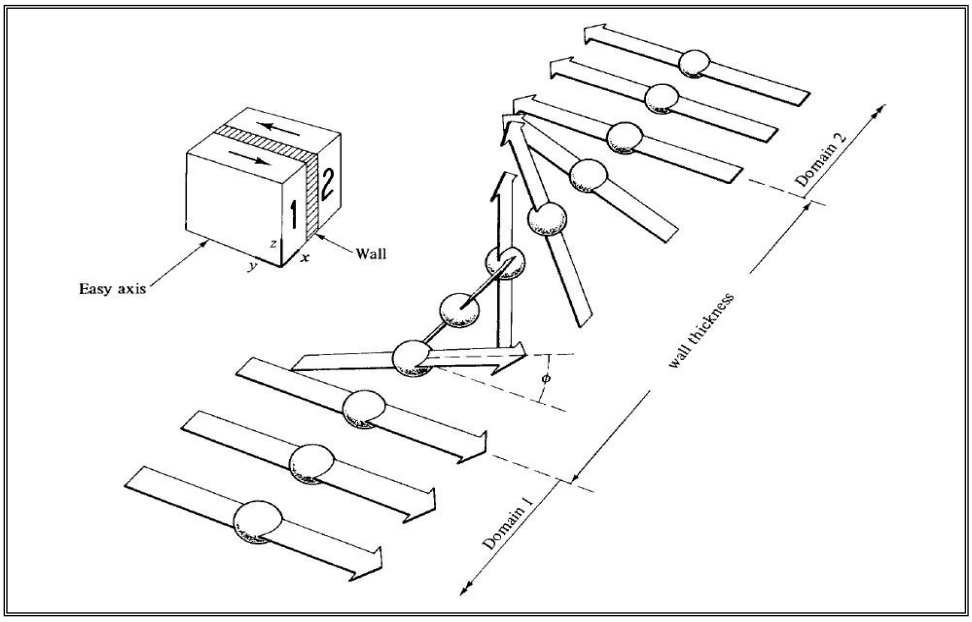

Figure 1.1: The gradual change of magnetic moment directions across the domain walls [9].

As an external magnetic field is applied, the domains change shape and size by the movement of domain walls. Schematic domain structures are represented in the insets (labeled U through Z) at several points along the B-H curve in Figure 1.2. Initially, the moments of the constituent domains are oriented randomly such that there is no net magnetization (M) or B field. As the external field is applied, the domains, that are oriented in direction of the applied field (or nearly aligned with the field), will grow at the expense of those which are unfavorably oriented. This growth will continue with the increasing field strength until the whole sample becomes a single domain, which is nearly aligned with the field. Saturation will occur (at Z) when this domain becomes aligned with the field [5].

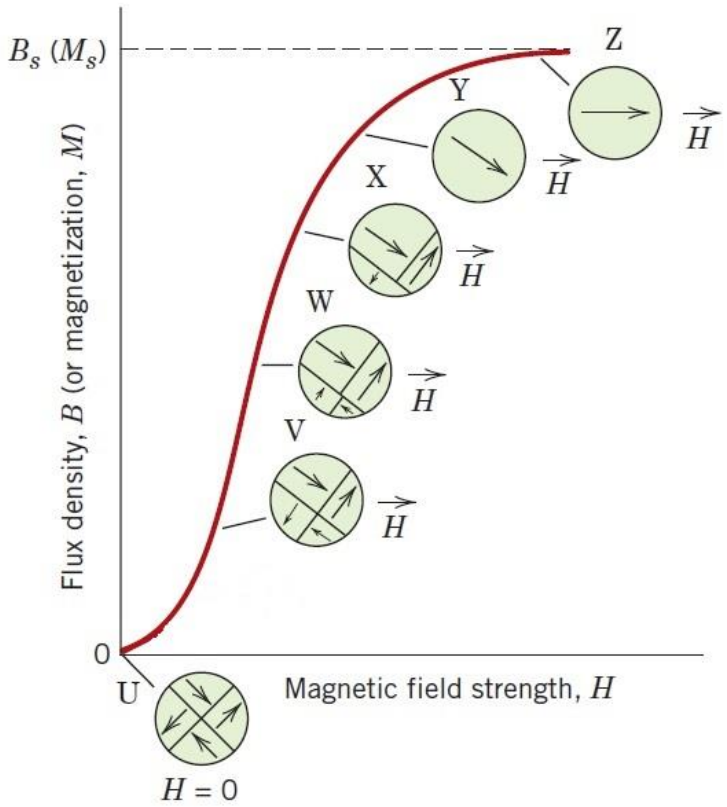

Figure 1.2: B-H behavior for an un-magnetized ferromagnetic or ferrimagnetic material [5].

At the point of saturation (S) in Figure 1.3, an external magnetic field is applied in the opposite direction, the field does not retrace its original path and a hysteresis loop will result, in which the B field lags behind the applied H field, or decreases at a lower rate. When the H field reaches zero point, the curve will have a certain value (point R on the curve). There exists a residual B field called remanence Br indicates that the material remains at the magnetized state in the absence of an external magnetic field. To reduce the B field in the sample to zero, an H field of magnitude $-H_c$ must be applied in the opposite direction of the original field. This value of H_c is called the coercivity. By increasing the reversed magnetic field as shown in Figure 1.3, then saturation will be achieved in the opposite sense corresponds (point S'). A second reversal of the field to the point of the first saturation (point

S) completes the symmetrical hysteresis loop and yield a negative remanence and positive coercivity [5,8].

Magnetic flux density versus the magnetic field strength for a Ferromagnetic material that is subjected to forward and reverse saturations (Points *S* and *S'*) Figure 1.3. The hysteresis loop is represented by the solid curve, while the dashed curve indicates the initial magnetization.

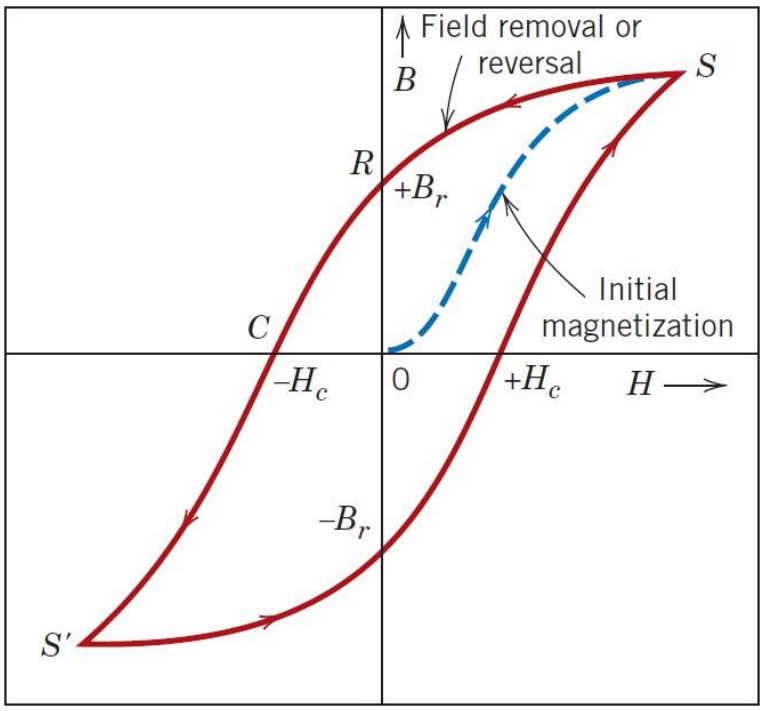

Figure 1.3: Hysteresis loop [5].

On increasing the temperature of the ferromagnetic specimen, the spontaneous magnetization starts decreasing smoothly until it vanishes at ($T=T_c$), see Figure 1.4, T_c is a specific point known as Curie temperature, indicating that the specimen undergoes a second order phase transition from ferromagnetic phase to paramagnetic phase. This transition occurs because of the thermal agitation due to the increasing in the thermal energy resulting in a random orientation of the spins [10].

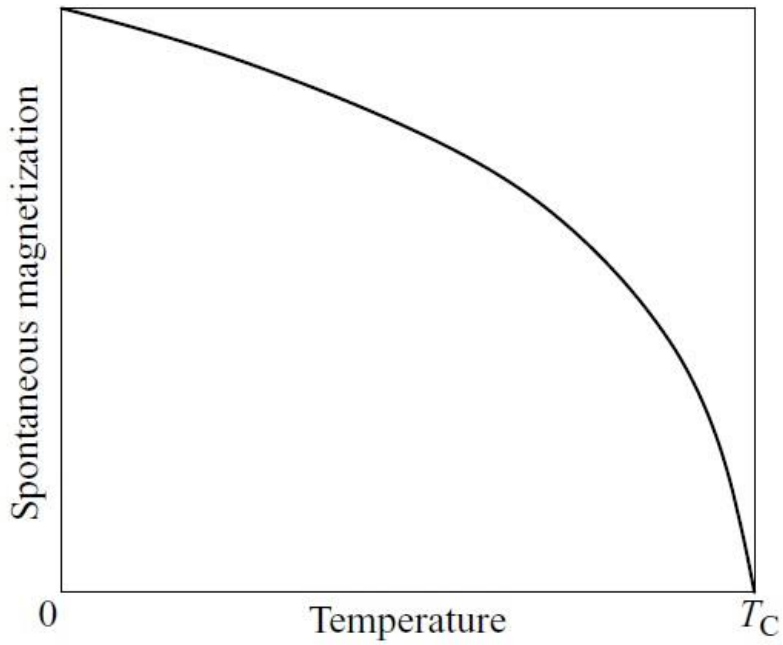

Figure 1.4: Variation of spontaneous magnetization with temperature in ferromagnetic materials [10].

1.3 Classification of Magnetic Materials

Based on the extent and nature of the interaction between electrons in the solid and an external magnetic field, it is possible to classify materials into five classes. Three of these classes are paramagnetic, diamagnetic, and antiferromagnetic solids that show almost no response to external magnetic fields [7]. In contrast, ferromagnetic and ferrimagnetic materials interact strongly with external magnetic fields and can be used in a variety of magnetic applications, including electrical transformers and information storage devices.

The property that quantitatively describes the material's response to an external field is its magnetic susceptibility (χ). If $|\chi| << 1$, The materials has a poor response to the external field; $|\chi| >> 1$, the material has a strong magnetic response.

Paramagnetic and diamagnetic characteristics appear in most common elements in the periodic table while ferromagnetism appears in the transition metal elements (TM) and rare

earth elements (RE) as shown in Figure 1.5, at room temperature [11]. In the next sections, the characteristics of these materials will be discussed in thorough details.

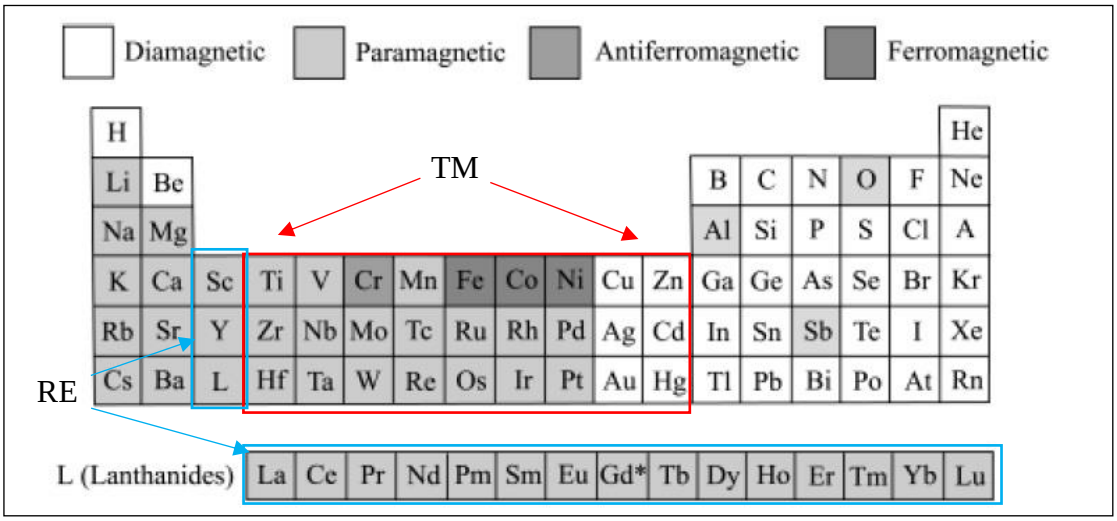

Figure 1.5: Periodic table shows the types of magnetic materials of all elements at room temperature [11].

1.3.1 Diamagnetic Materials

A diamagnetic is a substance that exhibits, a negative susceptibility (negative magnetization). Despite the fact that it is composed of atoms that has zero net magnetic moment, it reacts in a certain way to the applied field.

According to Ampere, the molecular currents are responsible for the magnetism in the solid materials. He compared the molecular currents to an electric current in a loop-shaped piece of wire, which gives rise to magnetic moment [5]. In order to understand the diamagnetism, an electric current has to be considered rather than molecular current. It was found by Lenz that a current is induced in a wire loop whenever a bar magnet is moved toward (or from) this loop. Thus The induced current causes a magnetic moment which is opposite to the applied magnetic field direction [9,12]. This effect is summed over all the electrons in the atom and each atom is considered to act independently of the others. All

materials have diamagnetic properties, but most of these materials have other magnetic behavior, which is more dominant than diamagnetism.

1.3.2 Paramagnetic Materials

Paramagnetism occurs when the atomic, ionic or molecular constituents have a non-zero magnetic moment. When an internal magnetic field is applied to the specimen, the magnetic moments will be aligned with the direction of the field as shown in Figure 1.7. Hence paramagnetic materials have a positive susceptibility. The diamagnetic moments are still present, but the aligned atomic moments have a greater magnitude than the induced diamagnetic moments [11].

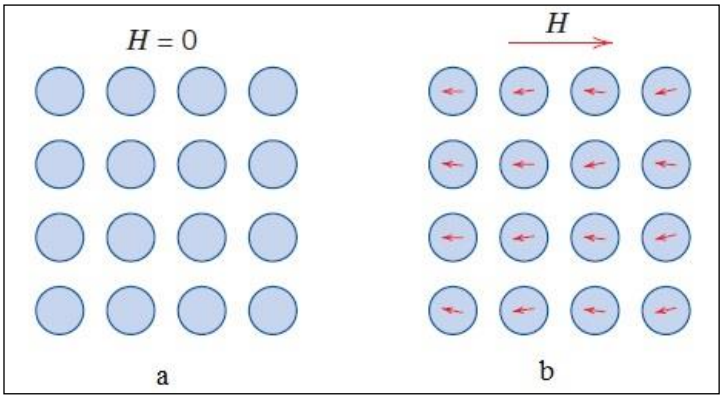

Figure 1.6: the atomic dipole for a diamagnetic material, (a) in absence of external field, and no dipoles exist. (b) In the presence of a field, dipoles induced and are aligned opposite to the field direction [5].

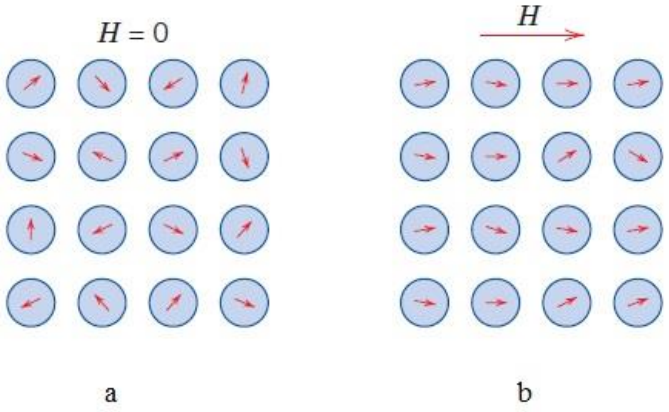

Figure 1.7: Atomic dipoles for a paramagnetic material, (a) with no applied magnetic field (b) with magnetic field [5].

The spin paramagnetism is slightly temperature dependent. It is a very weak type of magnetic behavior, which occurs in some metals, salts of the transition metals as well as rare earth metals and their salts and oxides. Curie- Weiss Law, which describes the magnetic susceptibility, in the paramagnetic region above the Curie point, can explain the temperature dependence of many paramagnetic materials that [6]:

$$\chi = \frac{C}{T - T_C} \qquad (1.2)$$

here, C is Curie constant depends on the material's type; T is absolute temperature, and T_c is the Curie temperature. This formula is a general of Curie's Law and it is valid only above the Curie temperature. Below T_c, the atomic magnetic moments tend to align in the same direction, which will induce a spontaneous magnetization and the material will be in ferromagnetic phase [13]. The spontaneous magnetization below the Curie temperature arises from an internal magnetic field called the Weiss molecular field, this field is proportional to the magnetizations of small domains in the material.

The main properties of paramagnetic materials may be summarized as follows [12]

1- When paramagnetic materials are placed in a magnetic field they obtain a slight value of magnetization in the direction of the applied magnetic field.

2- Paramagnetic materials show a positive, but small magnetic susceptibility about 10^{-6}.

3- In non-uniform magnetic field, the paramagnetic materials are attracted towards the strong region of magnetic field.

4- According to Curie's Law, The paramagnetic susceptibility is strongly dependent on temperature.

1.3.3 Ferromagnetic Materials

The characteristic feature of ferromagnetism is represented by the spontaneous magnetization property M, which is due to the alignment of the magnetic moment located on an atomic lattice. Weiss investigated ferromagnetism in term of a huge internal "molecular field" proportional to the magnetization [6].

It is well known that many paramagnetic materials, below a critical temperature, present alignment even in the absence of applied magnetic fields. These materials can also be considered as ferromagnetic materials. When an external magnetic field is applied to a ferromagnetic material, the material gets strongly magnetized and retains the magnetization in the material even when the external field is removed. Saturation magnetization can also be achieved by applying a small magnitude of external field 10 A/m. There are many materials that show a ferromagnetic property such as transition or irosn group element (e.g. Fe, Ni, Co), and rare earth group elements (e.g. Gd or Dy), shown in the periodic table in Figure 1.5 besides many other compounds and alloys [5,12,14].

Figure 1.8, shows the mutual alignment of magnetic dipoles for a ferromagnetic material, which does not exhibit any applied magnetic field [5].

When a ferromagnetic material is heated up to its critical temperature (Curie point), the magnetic dipoles will obtain thermal energy, which will increase the thermal agitation of these dipoles and hence, rotating them in a random way. This disorder of the magnetic moments is the paramagnetic phase. Different ferromagnetic materials have different values of Curie temperature, few of them are shown in table 1.1 [8].

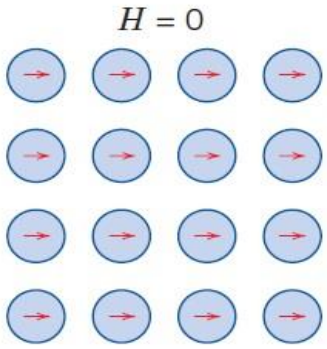

Figure 1.8: Ferromagnetic ordering in the absence of external field [5].

Table 1.1: Curie's Temperature for different ferromagnetic materials [8].

Material	*Curie temperature*
Iron	770 °C
Nickel	358 °C
Cobalt	1130 °C
Gadolinium	20 °C
Terfenol	380–430 °C
$Nd_2Fe_{14}B$	312 °C
Alnico	850 °C
$SmCo_5$	720 °C
Hard ferrites	400–700 °C
Barium ferrite	450 °C

1.3.4 Antiferromagnetic Materials

Antiferromagnetism is a mysterious magnetic order, in which a crystal lattice is subdivided into two or more atomic sublattices, which order in such a way that their net magnetization is equal to zero [6].

When investigating the antiferromagnetic behavior of the magnetic moments, it has been found that the neighboring spins are aligned antiparallel to each other so that their magnetic spins cancel each other, therefore it shows a very small positive susceptibility that is ranged from 10^{-5} to 10^{-2}. The theory of antiferromagnetism is mainly developed by Neel in which he applied molecular field to the problem [9,15].

Manganese oxide (MnO), Figure 1.9, is one of the materials that reveal an antiferromagnetic behavior. O^{-2} ions have no magnetic moment, since there is a total cancellation of both spin and orbital moment. However, the Mn^{+2} ions have a magnetic moment which mostly originates from the spin moment. These Mn^{+2} ions are arranged in the crystal structure in order for the adjacent ions to be antiparallel [5].

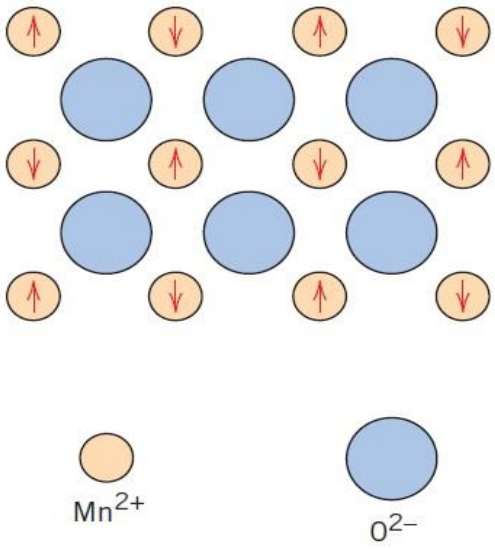

Figure 1.9: Schematic representation of antiparallel alignment of magnetic moments for antiferromagnetic manganese oxide [5].

Antiferromagnetic susceptibility varies with temperature as shown in Figure 1.10. As the temperature decreases, χ increases that it goes through a maximum point which is a critical temperature called Neel temperature T_N and usually it is less than room temperature, which indicates that with the appropriate measurement, a given paramagnetic material could be antiferromagnetic at low temperatures [9,15].

Weiss's theory explains the temperature dependence of the susceptibility by understanding the magnetic ordering. Before the publication of Neel's classic paper, it was known experimentally that the susceptibility of antiferromagnets depends on the temperature, as shown in Figure 1.10 [6]. For temperatures greater than a critical one, the

susceptibility follows the paramagnetic Weiss's law but with a negative value of θ as shown in Eq. (1.3). Therefore, ferromagnets and antiferromagnets are akin at high temperatures, that:

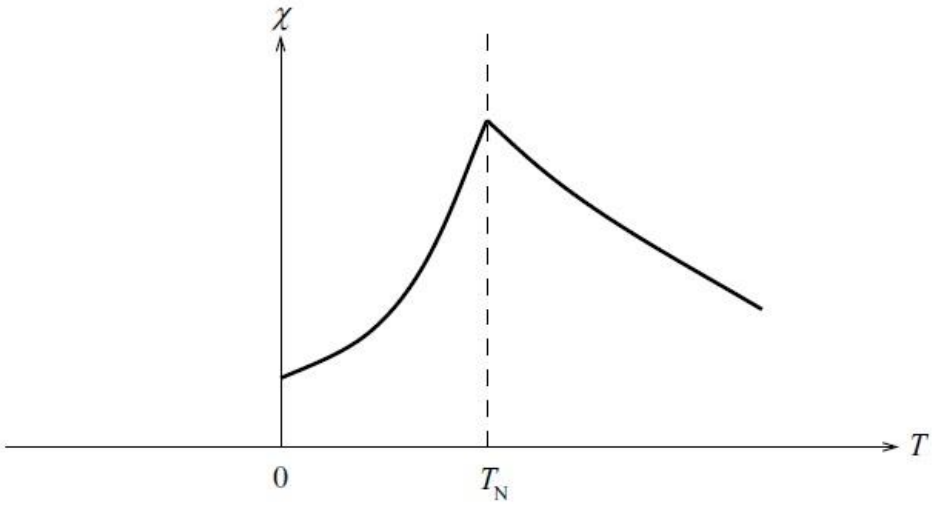

Figure 1.10: Temperature dependence of susceptibility for antiferromagnetic materials [10].

$$\chi = \frac{C}{T-(-\theta)} \tag{1.3}$$

Below the critical temperature, Neel temperature, the system becomes ordered. Therefore, the susceptibility decreases with decreasing temperature because of the tendency for the antiparallel alignment increases. A microscopic view is shown in Figure 1.11, for antiferromagnetic atomic moments, two different sublattices are noticed A-site and B-site. A molecular field theory takes accounts of only the antiparallel interaction between the A-site and B-site predicts that, $\theta/T_N = 1$. Table 1.2 shows that this is rarely the case because of the interactions within each sublattice [10,11].

Table 1.2: Some antiferromagnetic materials [11]

Substance	Paramagnetic Ion Lattice[a]	Transition Temperature T_N (K)	Curie–Weiss θ (K)	$\frac{\theta}{T_N}$	$\frac{\chi(0)}{\chi(T_N)}$
MnO	fcc	122	610	5.0	0.69
MnO_2	bct	84	–	–	0.93
α-MnS	fcc	154	465	3.0	0.82
β-MnS	fcc	155	982	6.3	–
MnTe	hex. layer	307	690	2.25	–
MnF_2	bc tetr.	67	82	1.24	0.76
FeF_2	bc tetr.	79	117	1.48	0.72
$FeCl_2$	hex. layer	24	48	2.0	<0.2
FeO	fcc	198	570	2.9	0.8
α-Fe_2O_3	rhomb.	950	2000	2.1	–
FeS	hex. layer	613	857	1.4	–
$CoCl_2$	hex. layer	25	38.1	1.53	–
CoF_2	bct	40	53	1.3	–
CoO	fcc	291	330	1.14	–
$NiCl_2$	hex. layer	50	68.2	1.37	–
NiO	fcc	525	~2000	~4	–
α-Mn	complex cubic	~100	–	–	–
Cr	bcc	308	–	–	–
CrSb	hex. layer	723	550	0.76	$\sim\frac{1}{4}$
Cr_2O_3	rhomb.	307	485	1.58	–
$FeCO_3$	complex	35	14	0.4	$\sim\frac{1}{4}$
$CuCl_2 \cdot 2H_2O$	rhomb.	4.3	5	1.2	–

1.3.5 Ferrimagnetic Materials

In a ferrimagnet, the magnetic moment for one type of ion in lattice site aligned antiparallel to those of ions on another lattice site. Because the magnetic moments are not at the same magnitude, they only partially cancel each other, which means that the material has a net magnetization. Ferrimagnetism has several similarities to ferromagnetism in that the mutual alignments between magnetic dipoles produce a net magnetic moment even in the absence of an applied field [16]. The difference between magnetic dipoles alignment of the ferromagnetism, antiferromagnetism, and ferrimagnetism is demonstrated (see Figure 1.11).

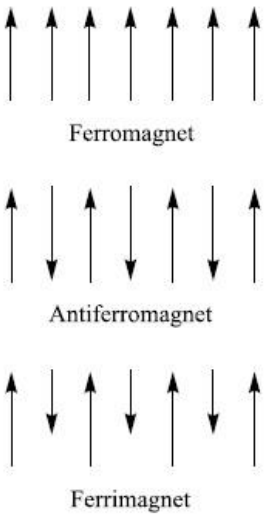

Figure 1.11: Magnetic moments spin arrangements for a ferromagnet, an antiferromagnet and a ferrimagnet [10].

A necessary condition for the appearance of ferrimagnetic arrangement is the presence of negative exchange interaction among the magnetic ions (atoms) associated with the different sublattices. Ferrimagnetism appears not only in crystalline magnetic materials but also in amorphous ones e.g. in alloys, in the temperature range from 0 to Neel point T_N [17].

A large number of ferrimagnets are known; the main class is the ferrites. There are three types of ferrites: cubic (spinal), hexagonal and garnet. Cubic ferrites have a general formula $MO.Fe_2O_3$, where M is a divalent metal like Mn, Ni, Fe, etc. Hexagonal ferrites have the formula $MO.6Fe_2O_3$ such as barium ferrite, $BaO_6Fe_2O_3$. Garnets are oxides with rare earth metals having general formula $5Fe_2O_3.3M_2O_3$. Here M stands for a trivalent element such as gadolinium, yttrium, terbium etc. table 1.3 shows some common ferrimagnetic materials [1,11]. It is already mentioned that ferrimagnets are similar to ferromagnets, which have a non-zero net magnetization below Curie's point (critical temperature) and does not show any magnetic ordering of the spins above this point and then it reveals a paramagnetic properties.

Table 1.3: Some common ferrimagnets with their critical and compensation temperatures [6]

	Sublattices	T_c (K)	T_{comp} (K)
Fe_3O_4	8*a*;16*d*	856	
YFe_5O_{12}	16*a*;24*d*	560	
$BaFe_{12}O_{19}$	2*a*,2*b*,4*f*1,4*f*2,12*k*	740	
$TbFe_2$	8*a*,16*d*	698	
$GdCo_5$	1*a*,2*c*,3*g*	1014	287

Nevertheless sometimes, there is a temperature below the critical temperature, at which the sublattice magnetizations are equal in magnitude having antiparallel arrangements produces zero net magnetization. This temperature is known as compensation point. Figure 1.12 illustrates the difference in magnetization and susceptibility between ferromagnets and ferrimagnet with respect to temperature [6,18].

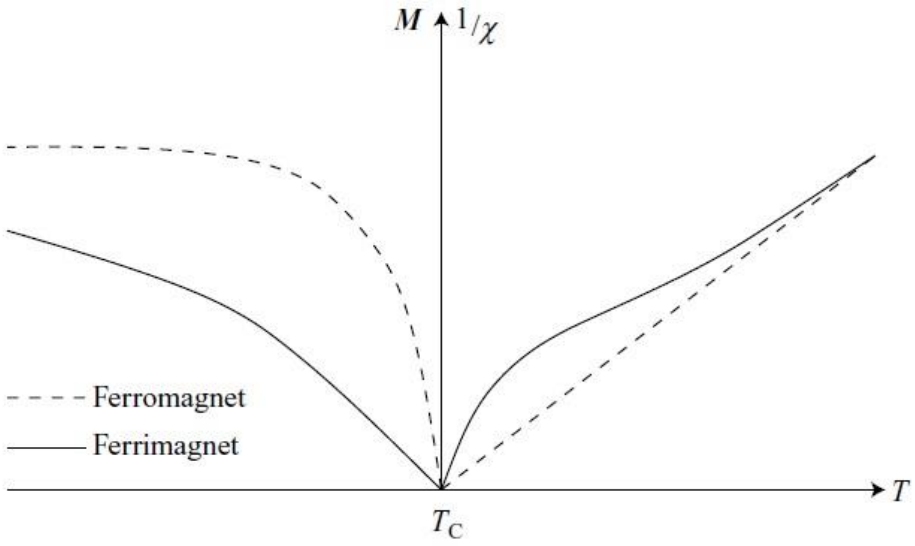

Figure 1.12: Comparison of magnetization and inverse susceptibility in typical ferromagnetic and ferrimagnetic materials [10].

1.4 Literature Review

In recent decades, the phenomenon of ferrimagnetism has been one of the intensively studied subjects in statistical mechanics and condensed matter physics, due to their wide range of applications in technologically important materials, unlike ferromagnets and antiferromagnets. Ferrimagnets have an important possibility of the existence, under certain conditions, of a compensation temperature where the total magnetization vanishes below the critical temperature. The existence of a compensation temperature is of great technological importance, since at this point only a small driven field is required to change the sign of the total magnetization in hysteresis loop. This property is very useful in thermomagnetic recording, electronic, and computer technologies [19].

The most simple and important model that deals with phase transitions for the ferromagnetic materials is the Ising model, which has been proposed by Ernest Ising in 1925. He studied only the one dimensional case and showed that his model does not behave as a ferromagnetic body [20,21].

Mixed Ising systems provide simple models, which can show ferrimagnetic ordering, and they may have compensation temperatures. The magnetic properties of these models have been studied by several methods such as Mean-Field, and an Effective Field theory, a Cluster Variational theory , Monte Carlo simulations, and so on [22].

T. Oguchi presented, in 1953 and 1955, an antiferromagnetic theory that based on Heisenberg model, which is a more efficient method than Weiss-Li's because the calculations can be taken out over all temperatures. In addition, he developed a simple and tractable theory, which includes short-range order effects. The perpendicular susceptibility of antiferromagnets below the Neel point was obtained [23,24].

B.R. Cooper in 1960 investigated the effect of large anisotropy on the thermal behavior of the sublattice magnetization and antiferromagnetic resonance frequency. By using

Oguchi method, he made some modifications to correct the molecular field approximation arising from pair correlation. The results were related to the experiments on FeF_2 where the anisotropy was comparable to the exchange energy [25].

In 1971 T. Ishikawa and T. Oguchi studied the phase transition for the spin systems described by a certain Hamiltonian at high-temperature series expansion method of the susceptibility in the absence of external field. The critical temperature T_C and the susceptibility were obtained for a 2-dimensinal square lattice, as a function of spin (S) and the anisotropy parameter (D) [26].

F. Y. Wu (1978) has determined the phase diagram of the spin one Ising system. He determined exactly the interaction of the ferromagnetic materials and schematic for antiferromagnetic intractions [27].

T. Kaneyoshi et al. in 1988 studied the magnetization curves for a mixed spin-1/2 and spin-1 Ising ferrimagnetic system with different transverse fields. They found the usual temperature dependence of magnetization and a compensation point is induced by the difference in transverse fields [28].

In 1991, by using the exact spin identities and the differential operator technique, T. Kaneyoshi et al. [29] developed a new effective field theory for the Blume-Capel model with a high spin S value. The phase diagrams for S=3/2 and S=2 were examined. Their predicted results show that their spin-3/2 model did not have a tricritical behavior, but spin-2 model did have a tricritical point.

M. Jascur and T. Kaneyoshi in 1995 studied the transition temperatures of a periodic bilayer system consist of two layer of spin-1/2 A atoms, two layers of spin-3/2 B atoms by using effective field theory. The effects of different crystal fields in the B layers and disordered interfaces on the transition temperature were revealed. They had obtained some

interesting phenomena depending on the different values of crystal fields and exchange interactions [30].

The effective field theory with correlations has been carried out by A. Bobak and M. Jurcisin in 1996, to examine the magnetic properties of a diluted mixed spin-1/2 and spin-3/2 Ising ferrimagnetic systems with coordination numbers, z=3 and 4. The results have showed that the presence of the compensation temperatures does not depend only on the magnitude of spins, but also on the crystal structure [31].

In 1997, researchers also investigated the phase diagrams and magnetization curves of the site-diluted mixed spin-1 and spin-3/2 Ising ferrimagnet on the honeycomb lattice by the use of effective-field theory with correlations. The considered system appears to have the possibility of three compensation points and some characteristic behaviors in the thermal variation of total magnetization not predicted by the Neel theory of ferrimagnetism [32].

M. Jascur in 1998 obtained exact solutions for the phase diagrams, compensation temperatures and magnetization curves of a decorated ferrimagnetic Ising model on the square lattice and discussed the results [33].

A. Bakchich and M. El. Bouziani in 1999 used both of mean field approximation and renormalization-group techniques, as a function of the ratio R of bulk and surface interactions and the ratio D of bulk and surface crystal fields. Various types of phase diagrams have been determined for the three dimensional semi-infinite ferromagnetic spin-3/2 Blume-Capel model [34].

A. Dakhama and N. Benayad in 2000 suggested an exactly solvable mixed spin-1/2 and any arbitrary spin-S (S>1/2) Ising ferrimagnetic model. Although the system with only an antiferromagnetic interactions J between pairs of nearest-neighbor spins and crystal fields does not undergo a compensation point. However the system with additional interactions

between spins does. At last, they have discussed the origin of compensation phenomenon [35].

In the same year Y. Nakamura et al. studied the magnetic characteristics of a diluted mixed spin-2 and spin-5/2 ferrimagnetic Ising model by using the effective-field theory taking the correlation between spins into account. The effects of transverse fields and concentration of magnetic atoms on the magnetic properties have been investigated numerically [36].

O.F. Abubrig et al. in 2001 have studied the mixed spin-1 and spin-3/2 Ising ferrimagnetic system with different anisotropies by using MFA based on Bogoliubov inequality for Gibbs free energy. The main phase diagrams have been obtained in the temperature-anisotropy plane. Besides, the presence and dependence of the compensation points on the crystal field have been investigated [37].

In 2003, Wei Jiang et al. introduced an effective field theory for a mixed spin-1 and spin-3/2 with different anisotropies in a transverse field of a honeycomb lattice. The calculation of the temperature dependence of total magnetization have been examined to determine the phase diagram of the transition temperatures. Some interesting phenomena occurred, such as the presence of two tricritical points and the existence of the two compensation points [38].

Guang-Shan and Hai-Qing (2004) examined the quantum phase transitions in the mixed spin Heisenberg model with single-ion anisotropy on a bipartite lattice. The model has a unique ground state when the total spin-z component $S_z=0$ and the single-ion anisotropy energy is positive, but when the single ion anisotropy energy is negative and favors the longitudinal spin direction, the general ground state becomes doubly degenerate [39].

E. Albayrak and Ali Yigit (2006) used the exact recursion relations on Bethe lattice in order to study the critical behavior of the mixed spin-3/2 and spin-5/2 Blume-Capel Ising ferrimagnetic system. The phase diagram with equal strength of single-ion anisotropy has

been examined. The system experiences first- and second-order phase transitions. For a certain values of crystal fields, the system showed a compensation behavior [40].

J. Oitmaa and I.G. Enting (2006) used high- and low- temperature expansions to study the phase diagram of a ferrimagnetic mixed-spin S=(1/2,1) Ising model on the square lattice. The results showed a first order phase transition for large negative anisotropy values. The model with nearest neighbor interactions only, does not appear to have a ferrimagnetic compensation point [41].

A. Benyoussef et al. (2007) examined the magnetic properties of a decorated ferrimagnetic mixed spin-1/2 and spin-1 Ising model consisting of two sublattices A and B by the use of mean field approach. For the decorated ferrimagnetic square lattice, the transition and compensation temperatures have been investigated [42].

A. Bobák et al. (2010) analyzed the effects of the exchange interactions and crystal fields on the magnetic susceptibility of the mixed spin-1 and spin-1/2 Heisenberg model by using the Oguchi approximation on simple cubic lattice with coordination number z= 6. It was also discussed the difference between the behaviors of the magnetic susceptibility of the Heisenberg and Ising model [43].

Deviren and Keskin in 2010 studied the dynamic phase transitions and the dynamic compensation temperatures, by using MFA, in the mixed spin-3/2 and spin-5/2 Ising system with single-ion anisotropy under the effect of magnetic field as a function of time on a hexagonal lattice. The thermal behavior of the dynamic sublattice and total magnetizations have been tested to obtain the dynamic phase transition and compensation temperatures as well as characterizing the nature of the transitions [44].

Espriella and Buendia in 2011 have performed Monte Carlo simulations to examine the magnetic characteristics of a mixed spin-3/2 and spin-5/2 Ising model. When the antiferromagnetic interactions are included in the Hamiltonian, with crystal field

interactions, the system presents compensation points in a certain range of values. The finite temperature phase diagram of the system have been calculated and it is found that the presence of compensation points depends on the strength of the ferromagnetic interactions between 3/2-spins [45].

J.S. da Cruz et al. (2013) studied the effect of two different values of crystal fields in the phase diagram and in the compensation temperature of a mixed spin-2 and spin-5/2 Ising ferrimagnetic system. The mean field theory has been used based on Bogoliubov inequality for gibbs free energy. By graphing the temperature versus crystal field plane, the phase diagram exhibit a tricritical behavior. The critical and compensation temperature is proportional to the single-ion anisotropy [46].

Gulistan Mert (2015) used the Oguchi's method to examine the thermodynamic characteristics of spin-1/2 Heisenberg ferromagnetic system on the simple cubic lattice. The influences of the exchange of the second-nearest-neighbor interactions on the magnetization, internal energy, heat capacity, entropy and free energy of the Heisenberg ferromagnet were considered. The ordinary ferromagnetic magnetization curves have been obtained and it is predicted that the critical temperature is proportional to the second-nearest-neighbor exchange interaction [47].

Xiaoling Shi et al. (2016) investigated the compensation behavior in molecular-based ferrimagnet $AFe^{II}\ Fe^{III}\ (C_2\ O_4)_3$ described by a mixed spin-2 and spin-5/2 ferrimagnetic Ising model within the effective field theory on a honeycomb lattice. By comparing their results with previous data obtained by the MFA, their results show a good improvement over the MFA results [48].

J. D. Alzate-Cardona et al. (2017) Studied the magnetic characteristics of a mixed spin $\mu=3/2$ and spin $\sigma=5/2$ Ising ferrimagnetic system in a graphene layer by Monte Carlo simulations. The effects of the exchange next-nearest neighbors interactions and single-ion

anisotropy on the critical and compensation behavior of the system have been examined. For a system with given values of ion anisotropy and constant exchange interaction, a compensation point only exists if the values of the spins $|\sigma|>|\mu|$ and J_s is higher than a certain value [49].

M. Ertas and A. Yilmaz have investigated the dynamic magnetic hysteresis properties of mixed spin ferrimagnetic Ising system that contains spin-3/2 and spin-5/2 in 2018. They have studied the effect of temperature, crystal-field and frequency on the hysteresis behavior of the considered system by using dynamic effective-field theory on square lattice. A single hysteresis loop, remanent magnetization and coercive field have been obtained [50].

The mixed spin-1 and spin-3/2 Ising ferrimagnetic model under the effect of different single-ion anisotropies has been studied by J. R. V. Pereira et al. Monte Carlo simulation has been applied to the considered system for square lattice. The system revealed only second-order phase transition unlike the results obtained by MFA. Their system also showed multicompensation temperatures for appropriate values of anisotropy [51].

1.5 Aims of the study

1. Investigation of the mixed spin-3/2 and spin-5/2 Blume-Capel Ising system within a developed Oguchi Approximation (OA).
2. Studying the magnetic properties of the Blume-Capel Ising system for sc and fcc lattices.
3. Examining the effects of the magnetic anisotropies (i.e. crystal field) on the induction and location of spin compensation temperatures.
4. Investigation of the free energy of the system at low temperatures.

1.6 Thesis Outline

The outline of this thesis was arranged as follows; Chapter one presents an introduction and literature review including classification of magnetic materials. Chapter two contains the fundamentals of magnetism. The utilized model that has been solved by a developed Oguchi Approximation is included in chapter three. Chapter four is organized for results and discussion. Finally, the conclusions and future works are included in chapter five.

CHAPTER TWO

Theory of Magnetism

2.1 Introduction

This chapter explores the origin of magnetic moment and theories of magnetic behavior of materials. It is namely the arrangement of magnetic moments within the material. These theories provide the useful mathematical models of the magnetic characteristics including order-disorder transitions such as Curie temperature and the compensation point [8].

These models are important to give a reasonable explanation of some phenomena like the appearance of spontaneous magnetization because of the parallel arrangement of all spins in the specimen. There could be an antiparallel arrangement of the spin, which also could result a spontaneous magnetization [15]. Both of these cases will be discussed in addition to the models that influence the rotation of the magnetic spins in different conditions.

2.2 Magnetic Moments of Electrons

Electrons have orbital motion around the nucleus which could be similar to the current in a loop of wire having no resistance; both are resembles a circulation of charge. Because of this motion, magnetic moment of an electron may be calculated by [9]:

$$m = (area\ of\ loop)(current) = AI \qquad (2.1)$$

where m is the magnetic moment, the size and shape of the orbit and the electron velocity must be known to be able to evaluate m. In Bohr Theory of the atom, the electron velocity υ and the circular orbit is r. in cgs units, e is the charge on the electron in esu and c is the velocity of light, so e/c is the charge in emu. However, in SI units the electronic charge is measured in coulombs. The current or charge passing through a given point per unit time, is then $(e/c)(\upsilon/2\pi r)$ (cgs) or $(ev/2\pi r)$ (SI), that is to say [9]:

$$m(orbit) = \pi r^2\left(\frac{ev}{2\pi rc}\right) = \frac{evr}{2c}(cgs) \quad or \quad = \pi r^2\left(\frac{ev}{2\pi r}\right) = \frac{evr}{2} \qquad (2.2)$$

an additional assumption of the theory is that the angular momentum of the electron must be an integral multiple of $h/2\pi$, where h is Planck's constant. Therefore,

$$mvr = n\frac{h}{2\pi} \tag{2.3}$$

where m is the mass of the electron. Combining these relations (2.2) and (2.3), magnetic moment of the electron in the first orbit can be obtained (n=1) [9],

$$m(orbit) = \frac{eh}{4\pi mc}(cgs) \quad or \quad = \frac{eh}{4\pi m}(SI) \tag{2.4}$$

The spin of the electron is a universal property of electrons in all states of matter at all temperatures. The electron behaves as if it is spinning about its own axis, and there is a definite amount of magnetic moment and angular moment associated with spin. It is found experimentally and theoretically that the magnetic moment, due to electron spin is $9.27 \times 10^{-24}\ A.m^2$ [9].

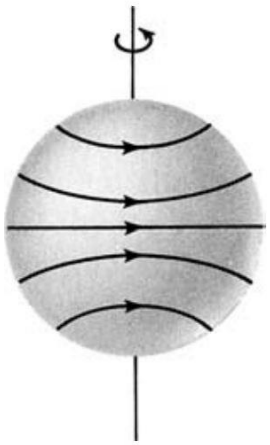

Figure 2.1: Visualization of electron spin [9].

Due to the motion in the first Bohr orbit, and the spin motion, the magnetic moment are exactly equal. Since it is a fundamental quantity, this amount of magnetic moment has a special name the Bohr magneton μ_B. So, it is considered as a natural unit of magnetic moment [9].

2.3 Magnetic Moment of Atoms

Atoms contain many electrons; each electron has its own orbit and spinning about its own axis. Both kinds of motion are a vector quantity that is associated with the magnetic moment, parallel to the axis of spin and normal to the orbit of motion, respectively. The magnetic moment of the atom is a vector sum of all its electronic moments, and two possibilities arise [9]:

1. The magnetic moments of all electrons are in opposite direction so that they cancel one another; hence, the atom has zero net magnetic moment and the result is a diamagnetic material.
2. The cancelation of electronic moments is only partial and the atom is left with a net magnetic moment. Such an atom is often referred to as a magnetic atom, that substances composed of atoms are para-, ferro-, antiferro, and ferromagnetic.

2.4 Weiss Theory of Magnetism

In 1907, Weiss introduced the first theory of an interacting magnetic system. He discussed that the cooperative ordering could be mimicked by assuming that each spin is subjected to an effective field called the molecular field and it is proportional to magnetization [52]. It is given by [15]:

$$H_m = wM \tag{2.5}$$

where w is the molecular field coefficient. The average magnetization under the effect of an external field H and a molecular field H_m is given by [15]:

$$M = \frac{Nm\int_0^{\pi} \exp\left(\frac{m(H+wM)}{k_B T}\cos\theta\right)\cos\theta\sin\theta d\theta}{\int_0^{\pi} \exp\left(\frac{m(H+wM)}{k_B T}\cos\theta\right)\sin\theta d\theta} \tag{2.6}$$

k_B is Maxwell Boltzmann constant, suppose that the parameter α is given by:

$$\alpha = \frac{m(H + wM)}{k_B T} \tag{2.7}$$

and $cos\,\theta = x$, then Eq. (2.6) becomes:

$$M = \frac{Nm\int_{-1}^{1} x\,\exp(\alpha x)dx}{\int_{-1}^{1}\exp(\alpha x)dx} \tag{2.8}$$

Using integration by part to solve (2.8), the solution for the numerator is:

$$\int_{-1}^{1}\exp(\alpha x)xdx = \frac{1}{\alpha}\left(\exp(\alpha)+\exp(-\alpha)\right) - \frac{1}{\alpha^2}\left(\exp(\alpha)-\exp(-\alpha)\right) \tag{2.9}$$

and the integral in the denominator is calculated to be:

$$\int_{-1}^{1}\exp(\alpha x)dx = \frac{1}{\alpha}\left|\exp(\alpha x)\right|_{-1}^{1} = \frac{1}{\alpha}\left(\exp(\alpha)-\exp(-\alpha)\right) \tag{2.10}$$

By substituting Eqs. (2.9) and (2.10) in Eq. (2.8):

$$M = Nm\left(\frac{\exp(\alpha)+\exp(-\alpha)}{\exp(\alpha)-\exp(-\alpha)} - \frac{1}{\alpha}\right) \tag{2.11}$$

The last equation can be reduced:

$$M = Nm\left(\coth\alpha - \frac{1}{\alpha}\right) \tag{2.12}$$

The function between the parentheses is known as the Langevin function and denoted by *L (α)*. So, Eq. (2.12) is put into the form as:

$$M = NmL(\alpha) \tag{2.13}$$

when $\alpha << 1$, the langevin function can be expanded as Tylor series:

$$L(\alpha) = \frac{\alpha}{3} - \frac{\alpha^3}{45} - .... \tag{2.14}$$

The terms of $L(\alpha)$ other than the first one will be neglected so that Eq. (2.12) will be:

$$M = \frac{Nm}{3}\alpha \tag{2.15}$$

Since Eq. (2.7) includes M, we can solve it with respect to M, and one has:

$$M = \frac{k_B T}{mw}\alpha - \frac{H}{w} \tag{2.16}$$

The solution of (2.13) can be obtained graphically. Figure 2.2 shows the curves of Eq.(2.13) and Eq.(2.16) with respect to α. Eq. (2.13) represents the langevin function as shown by curve (a) in Figure 2.2. Let us assume that H=0, such that H is an external field, and the spontaneous magnetization can be produced even at the absence of the external field. In this case, Eq. (2.16) becomes a straight line (b) through the origin. The solutions can be obtained by observing the intersection points O and S of curves (a) and (b). However, the point O produces an unstable solution, because if the magnetization has a non-zero value, such as S', near the origin, the state S' must rise along curve (b) (due to the definition of α, which entails that the state S' must always stay on the line (b)). The state of thermal equilibrium represented by curve (a) is above point S' until S' reaches S. Physically point O represents a completely random orientation of the spins. When there is some arrangement of spins by random processes, the alignment releases a non-zero molecular field, which leads to alignment that is more efficient. In contrast, point S represents a reasonable solution, because if the state changes from S to S", the equilibrium state is always near S.

Now let us speculate the dependence of spontaneous magnetization on temperature using the graphical solution mentioned earlier. At $T = 0$, the slope of the line (b) is zero, which indicates that the point S goes far to the right side, where $L(\alpha) = 1$ and $M = Nm$. This state is known as the saturation magnetization and denoted by M_S that [15]:

$$M_S = Nm \tag{2.17}$$

The derivative of the Langevin function with respect to (α) is given by:

$$\frac{dM}{d\alpha} = Nm\left(\frac{\partial L(\alpha)}{\partial \alpha}\right)_{\alpha=0} = \frac{Nm}{3} \tag{2.18}$$

Eq. (2.14) must be equal to the gradient of the line (b) in Eq. (2.16) at $T = Tc$, that:

$$\left(\frac{dM}{d\alpha}\right)_{\alpha=0} = \frac{K_B T_C}{mw} \tag{2.19}$$

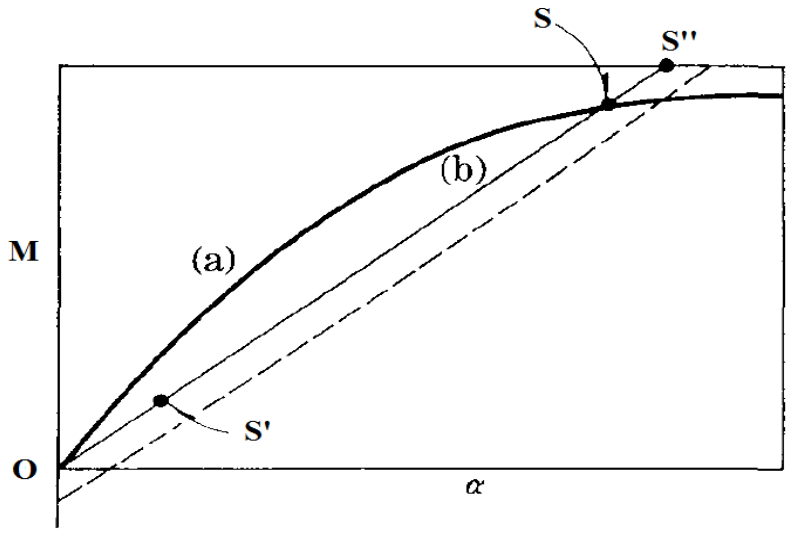

Figure 2.2: Graphical solution for spontaneous magnetization:
(a) Langevin function (b) Equation (2.16) [15].

Equating Eq. (2.18) with Eq. (2.19), we have:

$$T_C = \frac{Nm^2 w}{3k_B} \tag{2.20}$$

So far the effect of the external field has been neglected, because the external field is usually very weak compared to the exchange field i.e. very small influence on the magnitude of spontaneous magnetization. The second term in Eq. (2.16) gives the effect of the external field, which causes a shift of line (b) in Figure 2.2 downwards and hence a shift of the point S upwards, thus the magnetization M increases slightly. In this case, the susceptibility can be obtained [15]:

$$\chi = \frac{dM}{dH} = Nm\,\frac{\partial L(\alpha)}{\partial \alpha}\,\frac{\partial \alpha}{\partial H} \tag{2.21}$$

Moreover, from the definition of α in Eq. (2.7), one has:

$$\frac{\partial \alpha}{\partial H} = \frac{m}{k_B T} + \frac{mw}{k_B T} \cdot \frac{dM}{dH} \tag{2.22}$$

Substituting $\partial\alpha/\partial H$ from Eq. (2.21) and Eq. (2.22), results:

$$\chi = \frac{Nm^2 L'(\alpha)}{k_B (T - 3T_C L'(\alpha))} \tag{2.23}$$

where $L'(\alpha)$ is the differential function of $L(\alpha)$ with respect to α.

At very low values of temperature $T << TC$, $L'(\alpha)$ is very small that it gives a small value for the susceptibility Eq. (2.23). The susceptibility cannot be calculated without using high magnetic field. Hence, it is known as the high field susceptibility. However, when T reaches T_C, $L'(\alpha) = 1/3$, so that the denominator of Eq. (2.23) tends to vanish and the susceptibility approaches infinity. At $T > T_C$, the point S' remains near the origin in Fig. (2.2), where $L'(\alpha) = 1/3$, so that Eq. (2.23) becomes:

$$\chi = \frac{Nm^2}{3k_B (T - T_C)} \tag{2.24}$$

That is, the susceptibility is inversely proportional to the deviation of T from T_C, which is called the Curie-Weiss law. The susceptibility dependence on the temperature has been obtained as shown in Figure 2.3 [15].

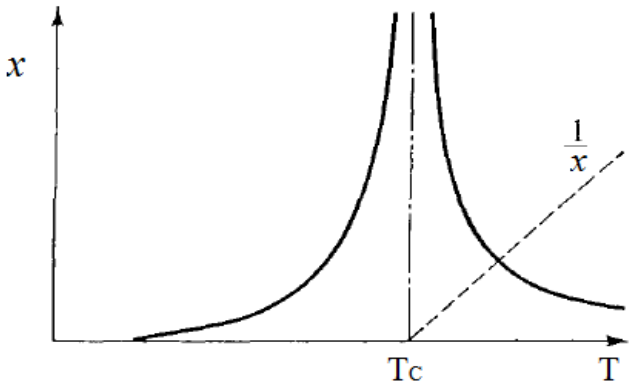

Figure 2.3: Magnetic susceptibility near the Curie temperature [15].

2.5 Magnetic Anisotropy

Experimentally, it has been found that the magnetization M prefers to situate along one or several axes in the magnetic solid. It takes an amount of energy to rotate to any other direction. This particular axis is called the easy axis. Therefore, the magnetic anisotropy can be defined as the energy needed to orientate the direction of magnetization from the easy to the hard direction [53].

Anisotropy has a great importance in the engineering of most commercial magnetic materials. A comprehensive knowledge of anisotropy is thus necessary for understanding these materials [9].

There are distinct types of anisotropies:

1- Crystal anisotropy (or magnetocrystalline anisotropy).

2- Shape anisotropy.

3- Stress anisotropy.

4- Anisotropy induced by

a. Magnetic annealing.

b. Plastic deformation.

c. Irradiation

5- Exchange anisotropy.

In this section, we will study the crystal anisotropy only because it is a substantial property to the materials, whilst all the others are extrinsic or “induced”.

2.5.1 Magnetocrystalline anisotropy

The magnetocrystalline anisotropy is the tendency of magnetization to align itself with a preferred crystallographic direction. The crystalline anisotropy can be observed by cutting a disk [110] from a single crystal of material as shown in Figure 2.4, and measuring the magnetization versus external field curves along the three high-symmetry crystallographic directions, ([110], [111], and [001]) included in the disk. A body center cubic Fe has the $< 100 >$ directions as its easy axis. In Ni, which is a face centered cubic; the easy axis is $< 111 >$. Note that the final value of the saturation magnetization is the same no matter which axis it is applied along, if the field is large enough, but the field required to reach the saturation value is clearly different in each case [10].

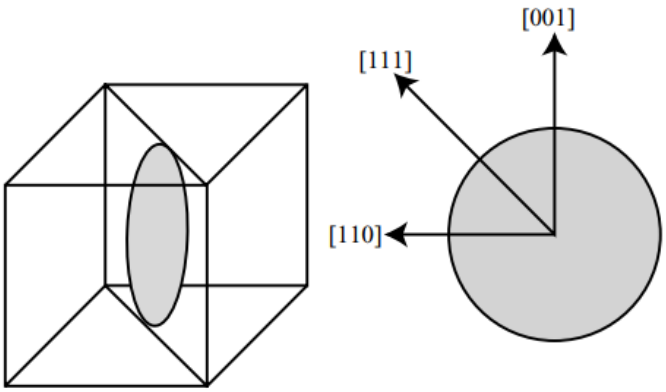

Figure 2.4 Preparation of a sample for measuring the magnetocrystalline anisotropy energy [10].

2.5.2 Physical Origin of Magnetocrysatlline anisotropy

Crystal anisotropy is mainly due to spin-orbit coupling which is some kind of interaction. Thus, the exchange interaction parameter between two neighboring spins could be considered as a spin-spin coupling. This coupling can be very strong, and acts to preserve the alignment or antialignment of the spins. However, the associated exchange energy is isotropic; it depends only on the angle between adjacent spins, and not on the direction of the spin axis associated to the spin lattice. The spin-spin coupling cannot therefore participate in crystal anisotropy.

The orbit-lattice coupling is also strong. This follows the fact that orbital magnetic moments are roughly entirely quenched. This means, in effect, that the orientations of the orbits are fixed very strongly to the lattice, because even large fields cannot change them.

There is also the coupling between the spin and the orbital motion of the electron. When an applied field attempts to change the spin of an electron, the orbit of that electron tends to be reoriented. Nevertheless, the orbit is strongly coupled to the lattice and therefore resists the attempt to orientate the spin axis. Now the anisotropy energy represents the energy that needed to rotate the spin system of a domain away from the easy axis and can be considered, as the energy required overcoming the spin-orbit coupling. These several relationships of the anisotropy are briefed in Figure 2.5 [9].

In most materials, the spin–orbit coupling is relatively weak, and so the magnetocrystalline anisotropy is not particularly strong. In rare-earth materials, however, the spin–orbit coupling is strong because rare-earth elements are heavy. Once magnetized, a large external field should be applied in the direction opposite to the magnetization to overcome the anisotropy and reverse the magnetization. Therefore, rare earth materials are often used in applications such as permanent magnets, where a large coercive field is required [10].

The magnitude of the crystal anisotropy mainly decreases with temperature more quickly than the magnetization, and it disappears at the Curie temperature. Due to the anisotropy strong effect on coercive field, the coercive field vanishes together with anisotropy. The combination of vanishing anisotropy and coercive field and nonvanshing magnetization leads to a maximum in permeability, especially the low field or initial permeability, which appears near the Curie point. This maximum point can be used as a simple method to find an approximate value of the Curie point [9].

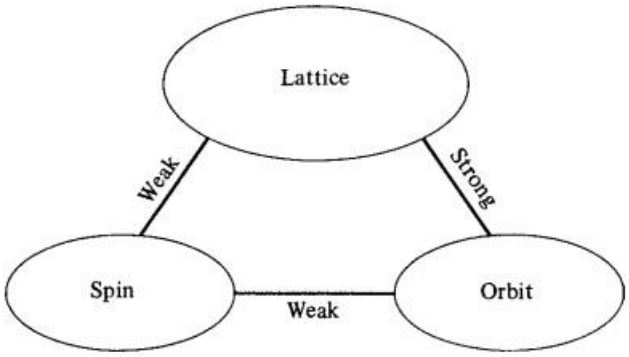

Figure 2.5 Strength of anisotropic energy between spin-lattice-orbit interactions

The single-ion anisotropy is essentially resulted from the electrostatic interactions of the orbitals containing the magnetic electrons with the potential in the atomic site that is created by the remaining of the crystal. This crystal-field interaction tends to stabilize a particular orbital, and by spin-orbit interaction, the magnetic moment is aligned in a particular crystallographic direction. In a ferromagnetic crystal, the contributions of all ions are summed to produce a set of macroscopic energy terms with appropriate symmetry. The sum is normal when the anisotropy axes of all sites localized in the unit cell. For example, a uniaxial crystal having $n = 2 \times 10^{28}$ ions, described by a spin Hamiltonian DS_z^2 with $D/K_B = 1K$ and $S = 2$ will have anisotropy constant equals to $nDS^2 = 1.1 \times 10^6\ J.m^{-3}$[6].

CHAPTER THREE

Theoretical Model

3.1 Introduction

The Ising model and its various variants are of the most extensively studied many-body problem. The reason is due to the fact that they can describe fairly well numerous physical systems, such as magnetic spin systems, binary alloys, lattice gas, and so on [54]. It is worth to note that the model is invented for the phase transition of ferromagnets at the Curie temperature. However, in the course of time it was realized that with only slight changes the model could also be applied to other phase transitions, like order-disorder transitions in binary alloys. Furthermore, the model may be applied to several modern problems of many-particle physics, for instance the description of so-called spin glasses.

3.2 Ising Model

Ising model is the simplest model that deals with the interaction among spins and it can show a phase transition such as the transition from ferromagnetism to paramagnetism. With Ising model, the system is considered as an array of N fixed points called lattice sites that form an n-dimensional periodic lattice (n=1,2,3). The geometric structure of the lattice may be square, cubic or hexagonal. A spin variable S_i (i=1, ….,N), which is a number that is either +1 or -1, is Associated with each lattice site. If $S_i = +1$, the ith site is said to have spin up, and if $S_i = -1$, it is said to have spin down. A set of numbers $\{S_i\}$ specifies a configuration of the whole system and the energy of the configuration is defined to be [55]

$$H\{S_i\} = -J\sum_{<ij>} S_i S_j - H_O \sum_{i=1}^{N} S_i \qquad (3.1)$$

where <ij> denotes a nearest-neighbor pair of spins. H_O is the external magnetic field. The first term indicates the cooperative behavior and the possibility of a phase transition. J is the exchange energy where J>0 favors parallel and J<0 favors antiparallel alignment of

spins for ferro-and antiferromagnetic behavior, respectively. For J=0 Eq.3.1 stands for the Hamiltonian of a paramagnet [56].

In 1925, Ising introduced simplest form of the Ising model that appears in one-dimensional lattice consisting of spin-1/2 atoms, with nearest-neighbor interaction in the absence of external field. However, he did not obtain a long-range order at any finite temperature. Yet, one may say that the Ising chain undergoes a phase transition at zero temperature [57].

The two dimensional Ising models in the absence of an external field has been solved exactly by Onsager in 1944 when he obtained a phase transition at a finite temperature [58]. After onsager's solution, the Ising model has been one of the most actively studied problems in statistical mechanics.

3.3 Blume-Capel-Model

The simplest spin model displays tricritical phase diagram in the absence of randomness is the Blume-Capel model. This model is used to simulate the thermodynamics of a variety of systems such as UO_2 [59], and it has been studied extensively with many mechanisms such as mean field approximation, position-sapce renormalization group, Monte Carlo simulations and other methods [60]. The Blume-Capel (BC) model includes two thermodynamic fields: the temperature T and the magnetic anisotropy (i.e., crystal field) D conjugates to $-S^2$, where S is the spin, which originally takes three values ±1 and zero [60].

3.4 Blume-Capel Ising Model

In principle, BC model is a spin-one Ising system, but it could be generalized to cover other combinations such as half-integer spin or mixed spin systems. Now let us examine

how a two undistinguishable spin-one BC Ising model can be formulated. The Hamiltonian of the BC Ising model is given by T. Kaneyoshi [61]:

$$H = -J\sum_{<ij>} S_i^z S_j^z - D\sum_i (S_i^z)^2 \tag{3.2}$$

where S_i^z takes the values ±1 and 0, and the first summation runs over all nearest-neighbor spins. J, (J>0; for ferromagnet J<0; for ferrimagnet, or antiferromagnet), is the exchange interaction and D is the crystal-field constant.

By using Maxwell Boltzmann statistics, one can obtain the thermal average of S_i^z i.e. m=$<S_i^z>$ as follows

$$< S_i^z >= \frac{\sum_i S_i^z e^{-\beta H}}{\sum_i e^{-\beta H}} \tag{3.3}$$

Substituting H in Eq. (3.3), we get:

$$< S_i^z >= \frac{\sum_i S_i^z e^{-\beta[-J\sum S_i^z S_j^z - D\sum (S_i^z)^2]}}{\sum_i e^{-\beta[-J\sum S_i^z S_j^z - D\sum (S_i^z)^2]}} \tag{3.4}$$

By putting βJ=t, and $\sum_i S_j^z = z < S_i^z > = zm$, one obtains:

$$< S_i^z >= \frac{\sum_i S_i^z e^{tzmS_i^z + \beta D(S_i^z)^2}}{\sum_i e^{tzmS_i^z + \beta D(S_i^z)^2}} \tag{3.5}$$

since i takes the values (±1, 0), then:

$$< S_i^z >= \frac{e^{tzm+\beta D} - e^{-tzm+\beta D}}{e^{tzm+\beta D} + e^{-tzm+\beta D} + 1} \tag{3.6}$$

By using the identity $e^x + e^{-x} = 2cosh(x)$ and $e^x - e^{-x} = 2sinh(x)$ Eq. (3.6) becomes

$$< S_i^z >= \frac{2\sinh(tzm)e^{\beta D}}{2\cosh(tzm)e^{\beta D} + 1} \tag{3.7}$$

$$< S_i^z >= \frac{2\sinh(tzm)}{2\cosh(tzm)+e^{-\beta D}} \quad (3.8)$$

when D→∞, $< S_i^z >$ become equals to $\tanh(tzm)$. In other words, when D takes a large positive value, the BC Ising model is reduced to the standard spin-1/2 Ising model [61].

3.5 Oguchi Approximation

Oguchi approximation (OA) is one of the effective field theories which is produced by Oguchi in 1955 to make a development upon the simple Mean-Field approximation [24]. In the Oguchi method, the interaction of a pair of nearest-neighbor spins say S_i and S_j, is treated exactly and the interactions of S_i and S_j with their neighboring spins are replaced by effective-field terms [62, 63], the Hamiltonian of the OA is given by.

$$H_{OA} = -JS_iS_j - JS_i\sum_l S_l - JS_j\sum_k S_k - H_o(S_i + S_j) \quad (3.9)$$

3.6 Identical particles

Let us take the simplest configuration, which is the spin-1 Ising system. Identical particles have $\sum_l S_l = \sum_k S_k = (z-1) < S_l >= (z-1)m$ where, $< S_k >=< S_l >= m$, m is the total magnetization of the crystal lattice, that:

$$H_{OA} = -JS_iS_j - J(z-1)mS_i - J(z-1)mS_j - \mathrm{g}\mu_B H_o(S_i + S_j) \quad (3.10)$$

or

$$H_{OA} = -JS_iS_j - J(z-1)m\big(S_i + S_j\big) - \mathrm{g}\mu_B H_o(S_i + S_j) \quad (3.11)$$

So,

$$H_{OA} = -JS_iS_j - (J(z-1)m + \mathrm{g}\mu_B H_o)(S_i + S_j) \quad (3.12)$$

where, g is Landé g-factor , μ_B is Bohr magneton = $9.274 \times 10^{-24}\ J/T$. Now, to find m we use Maxwell-Boltzmann statistics as follows

$$m = < \frac{S_i + S_j}{2} > = \; m = \frac{\sum\sum \frac{S_i + S_j}{2} e^{-\beta H_{OA}}}{\sum e^{-\beta H_{OA}}} \tag{3.13}$$

$$m = \frac{\sum\sum \frac{S_i + S_j}{2} e^{-\beta(-JS_iS_j - (J(z-1)m + g\mu_B H_o)(S_i + S_j))}}{\sum\sum e^{-\beta(-JS_iS_j - (J(z-1)m + g\mu_B H_o)(S_i + S_j))}} \tag{3.14}$$

The numerator of Eq. (3.14),

$$\sum_{S_i}\sum_{S_j} (\frac{S_i + S_j}{2}) e^{tS_iS_j + \beta(J(z-1)m + g\mu_B H_o)(S_i + S_j)}$$

can be found as,

$$= \sum_{S_j} (\frac{1+S_j}{2}) e^{tS_j + \beta(J(z-1)m + g\mu_B H_o)(1+S_j)} + (\frac{-1+S_j}{2}) e^{-tS_j + \beta(J(z-1)m + g\mu_B H_o)(-1+S_j)} \tag{3.15}$$

$$= e^{t + 2\beta(J(z-1)m + g\mu_B H_o)} - e^{t - 2\beta(J(z-1)m + g\mu_B H_o)} \tag{3.16}$$

Putting $h = J(z-1)m$ is the effective field assumed by Oguchi. Where $t=\beta J$, the denominator of Eq (3.14)

$$\sum_{S_i}\sum_{S_j} e^{tS_iS_j + \beta(h + g\mu_B H_o)(S_i + S_j)}$$

is evaluated as,

$$= e^{t + 2\beta(h + g\mu_B H_o)} + e^{-t} + e^{-t} + e^{t - 2\beta(h + g\mu_B H_o)} \tag{3.17}$$

By substituting Eqs. (3.16) and (3.17) in (3.14) the total magnetization for the spin-1 Ising system in Oguchi approximation is obtained.

$$m = \frac{e^{t + 2\beta(h + g\mu_B H_o)} - e^{t - 2\beta(h + g\mu_B H_o)}}{e^{t + 2\beta(h + g\mu_B H_o)} + e^{t - 2\beta(h + g\mu_B H_o)} + 2e^{-t}} \tag{3.18}$$

or

$$m = \frac{e^{t}\left(e^{2\beta(h+g\mu_B H_o)} - e^{-2\beta(h+g\mu_B H_o)}\right)}{e^{t}\left(e^{2\beta(h+g\mu_B H_o)} + e^{-2\beta(h+g\mu_B H_o)} + 2e^{-2t}\right)} \tag{3.19}$$

Then,

$$m = \frac{\sinh(2(z-1)tm + \beta g\mu_B H_o)}{\cosh(2(z-1)tm + \beta g\mu_B H_o) + e^{-2t}} \tag{3.20}$$

where t=βJ and $\beta = 1/K_B T$. T is the absolute temperature. To find the susceptibility of the system for identical particles we use the following relations [52]

$$\chi = \frac{\partial M}{\partial H_o}, \qquad \frac{M}{M_o} = m \tag{3.21}$$

where M is the total magnetic moment, and $M_o = Ng\mu_B$ is the saturation magnetization at T=0,

Then, $$\chi = \frac{\partial M_o m}{\partial H_o}, \tag{3.22}$$

$$\chi = Ng\mu_B \frac{\partial m}{\partial H_o} \tag{3.23}$$

taking the derivative of Eq. (3.20), one has:

$$\frac{\partial m}{\partial H_o} = \frac{[\cosh(x) + e^{-2t}]\cosh(x)[2(z-1)t\frac{\partial m}{\partial H_o} + \beta g\mu_B] - \sinh^2(x)[2(z-1)t\frac{\partial m}{\partial H_o} + \beta g\mu_B]}{[\cosh(x) + e^{-2t}]^2} \tag{3.24}$$

where $x = 2(z-1)tm + \beta g\mu_B H_o$.

$$\frac{\partial m}{\partial H_o} = \frac{\cosh^2(x)[2(z-1)t\frac{\partial m}{\partial H_o} + \beta g\mu_B] + e^{-2t}\cosh(x)[2(z-1)t\frac{\partial m}{\partial H_o} + \beta g\mu_B] - \sinh^2(x)[2(z-1)t\frac{\partial m}{\partial H_o} + \beta g\mu_B]}{[\cosh(x) + e^{-2t}]^2} \tag{3.25}$$

or,

$$\frac{\partial m}{\partial H_o} = \frac{[2(z-1)t\frac{\partial m}{\partial H_o} + \beta g\mu_B] + e^{-2t}\cosh(x)[2(z-1)t\frac{\partial m}{\partial H_o} + \beta g\mu_B]}{[\cosh(x) + e^{-2t}]^2} \tag{3.26}$$

when $x \ll 1$ then, $\cosh(x) = 1$ and $\sinh(x) = x$ then Eq. (3.26) becomes:

$$\frac{\partial m}{\partial H_o} = \frac{[2(z-1)t\,\frac{\partial m}{\partial H_o} + \beta g\,\mu_B][1+e^{-2t}]}{[1+e^{-2t}]^2} \tag{3.27}$$

$$\frac{\partial m}{\partial H_o} = \frac{[2(z-1)t\,\frac{\partial m}{\partial H_o} + \beta g\,\mu_B]}{[1+e^{-2t}]} \tag{3.28}$$

or,

$$\left[\frac{\partial m}{\partial H_o} + e^{-2t}\,\frac{\partial m}{\partial H_o} = 2(z-1)t\,\frac{\partial m}{\partial H_o} + \beta g\,\mu_B\right] \div \frac{\partial m}{\partial H_o} \tag{3.29}$$

Then,

$$\frac{\partial m}{\partial H_o} = \frac{\beta g\,\mu_B}{1+e^{-2t} - 2(z-1)t} \tag{3.30}$$

Taking the Taylor series expansion of e^{-2t} and substituting in Eq. (3.30)

$$e^{-2t} = 1 - 2t + 2t^2 - \frac{4t^3}{3} + \frac{2t^4}{3} ..... \tag{3.31}$$

So, Eq. (3.30) becomes:

$$\therefore \frac{\partial m}{\partial H_o} = \frac{\beta g\,\mu_B}{1+1-2t-2tz+2t} \tag{3.32}$$

$$\frac{\partial m}{\partial H_o} = \frac{\beta g\,\mu_B}{2-2zt} \tag{3.33}$$

Thus,

$$\chi = \frac{N\,(g\,\mu_B)^2}{2K_BT}\,\frac{1}{1-zt} \tag{3.34}$$

Since,

$$t = \beta J = \frac{J}{K_BT}, \quad C = \frac{N\,(g\,\mu_B)^2}{2K_B} \tag{3.35}$$

Eq. (3.34) becomes:

$$\chi = \frac{C}{T}\frac{1}{1-\frac{zJ}{K_B T}} \Rightarrow \chi = \frac{C}{T-\theta} \tag{3.36}$$

where $\theta = zJ/K_B$.

3.7 Distinguishable particles

The distinguishable particles system is considered here, where Oguchi method can be developed in the absence of the external field and the single-ion anisotropy is included. The mixed-spin ferrimagnetic Ising model, consists of three-dimensional sublattices S_i^A and S_j^B with spins $S_i^A = \pm 1/2, \pm 3/2$ and $S_j^B = \pm 1/2, \pm 3/2, \pm 5/2$ respectively. Here, the Oguchi method deals with central pair of neighboring atoms, and one can assume that the pair is coupled to the rest of the lattice through an effective field [24]. These assumptions are shown in Figure 3.1, which reveals only the atoms that contribute to an effective magnetic effect. The Hamiltonian of the system is given by Bobak et al. [64] Eq. (3.37).

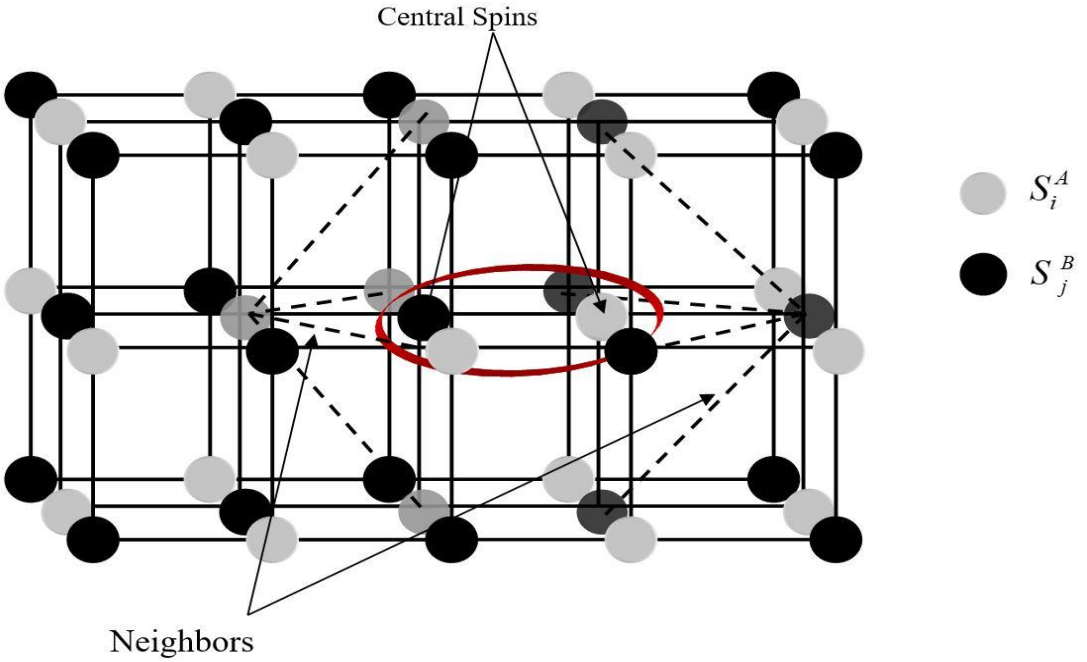

Figure 3.1: Scheme of a ferrimagnetic Ising system with two types of spins ($S_i^A = 3/2, S_j^B = 5/2$) for atoms A and B, respectively with coordination number $z = 6$ in the Oguchi representation.

$$H = -JS_i^A S_j^B - D_A(s_i^A)^2 - D_B(s_j^B)^2 - (h_i S_i^A + h_j S_j^B) \quad (3.37)$$

where the first term accounted for the spin-spin interaction and the second and third terms are the interaction of magnetic spins of atoms A and B with ion-anisotropies D_A and D_B, respectively. The last term is the effective field of Oguchi's assumption with $h_i = J(z-1)m_B$ and $h_j = J(z-1)m_A$. J is the exchange interaction among spins at sites i and j and for ferrimagnetic materials $J < 0$. z is the number of nearest neighboring spins and the sublattice magnetizations m_A and m_B are the thermal averages of S_i^A and S_j^B, respectively, i.e. $m_A = < S_i^A >$ and $m_B = < S_j^B >$. Calculating the Eigen values of the Hamiltonian Eq. (3.37), one can obtain the sublattice magnetization per site. D_A, D_B are the anisotropies, i.e., the crystal fields, acting on the spin-3/2 and spin-5/2 respectively.

The knowledge of the partition function (Z) allows us to identify the relations of thermodynamic quantities. Then, the free energy of the model is defined as [65],

$$F = -K_B T \ln Z \; ; \qquad Z = \sum e^{-\beta H} \quad , \quad (3.38)$$

where F is the free energy of the system given by Eq. (3.38). F determines the stability of the sublattice magnetization per site which is obtained by minimizing the free energy Eq. (3.38). It is worth noting that the ferrimagnetic case shows that the signs of sublattice magnetizations are different, and there may be a compensation point at which the sublattice magnetizations will cancel each other, hence, the total longitudinal magnetization vanishes [66],

$$m = \frac{1}{2}(m_A + m_B) = 0 \quad (3.39)$$

The sublattice magnetization of A atoms with spin-3/2 can be calculated by [67],

$$m_A = \frac{\sum S_i e^{-\beta H_A}}{Z_A}, Z_A = \sum e^{-\beta H_A} \quad (3.40)$$

With, $$H_A = -JS_iS_j - h_i\left(S_i + \frac{3}{5}S_j\right) - D_A S_i^2 \quad (3.41)$$

and for atoms B with spin-5/2, the sublattice magnetization is evaluated such that:

$$m_B = \frac{\sum S_j e^{-\beta H_B}}{Z_B}, Z_B = \sum e^{-\beta H_B} \quad (3.42)$$

with, $$H_B = -JS_iS_j - h_j\left(S_j + \frac{5}{3}S_i\right) - D_B S_j^2 \quad (3.43)$$

The compensation points, which are due to the different behaviors of sublattice magnetizations under the temperature changes, can be calculated by obtaining the crossing points between the absolute values of sublattice magnetizations $|m_A| = |m_B|$, at T_K or $m = |m_A| - |m_B| = 0$, where, sign m_A=-sign m_B, at T_K and $T_K < T_C$, by using Eqs. (3.41) and (3.40), so, we obtain the sublattice magnetization for atoms A:

$$m_A = \frac{1}{2}\left(\begin{array}{l} 3[a_1\sinh(g_1) + b_1\sinh(g_2) + b_2\sinh(g_3) + b_3\sinh(g_4) + \\ b_4\sinh(g_5)] + e^{-2\beta D_A}[a_2\sinh(h_1) - a_3\sinh(h_2) + b_3\sinh(h_3) \\ + b_4\sinh(h_4) + c_1\sinh(h_5) + c_2\sinh(h_6)] \end{array}\right) /$$

$$\left(\begin{array}{l} a_1\cosh(g_1) + e^{-\frac{15}{4}t} + b_1\cosh(g_2) + b_2\cosh(g_3) + b_3\cosh(g_4) + \\ b_4\cosh(g_5) + e^{-2\beta D_A}[a_2\cosh(h_1) + a_3\cosh(h_2) + b_3\cosh(h_3) + \\ b_4\cosh(h_4) + c_1\cosh(h_5) + c_2\cosh(h_6)] \end{array}\right) \quad (3.44)$$

where, $g_1 = 3\beta h_i$, $g_2 = 2.4\beta h_i$, $g_3 = 0.6\beta h_i$,

$$\left.\begin{array}{lll} g_4 = 1.8\beta h_i, & g_5 = 1.2\beta h_i, & h_1 = 2\beta h_i, \\ h_2 = \beta h_i, & h_3 = 1.4\beta h_i, & h_4 = 0.4\beta h_i, \\ h_5 = 0.8\beta h_i, & h_6 = 0.2\beta h_i, & \end{array}\right\} \quad (3.45)$$

and,

$$\left.\begin{array}{lllll} a_1 = e^{\frac{15}{4}t}, & a_2 = e^{\frac{5}{4}t}, & a_3 = e^{-\frac{5}{4}t}, & b_1 = e^{\frac{9}{4}t}, & b_2 = e^{-\frac{9}{4}t} \\ b_3 = e^{\frac{3}{4}t}, & b_4 = e^{-\frac{3}{4}t}, & c_1 = e^{\frac{1}{4}t}, & c_2 = e^{-\frac{1}{4}t} & \end{array}\right\} \quad (3.46)$$

and t=βJ, similarly, by using Eqs. (3.42) and (3.43) we obtain the sublattice magnetization for atoms B:

$$m_B = \frac{1}{2}\left(\begin{array}{l} 5[a_1\sinh(x_1)+a_2\sinh(x_2)+a_3\sinh(x_3)]+3e^{-4\beta D_B} \\ [b_1\sinh(y_1)+b_2\sinh(y_2)]+b_3\sinh(y_3)+b_4\sinh(y_4)]+e^{-6\beta D_B} \\ [b_3\sinh(z_1)+b_4\sinh(z_2)+c_1\sinh(z_3)-c_2\sinh(z_4)] \end{array}\right) /$$

$$\left(\begin{array}{l} a_1\cosh(x_1)+e^{-\frac{15}{4}t}+a_1\cosh(x_2)+a_3\cosh(x_3)+e^{-4\beta D_B} \\ [b_1\cosh(y_1)+b_{24}\cosh(y_2)+b_3\cosh(y_3)+b_4\cosh(y_4)]+e^{-6\beta D_B} \\ [b_3\cosh(z_1)+b_4\cosh(z_2)+c_1\cosh(z_3)+c_2\cosh(z_4)] \end{array}\right) \quad (3.47)$$

where,

$$\left.\begin{array}{llll} x_1 = 5\beta h_j, & x_2 = 3.3\beta h_j, & x_3 = 1.6\beta h_j, & y_1 = 4\beta h_j, \\ y_2 = \beta h_j, & y_3 = 2.3\beta h_j, & y_4 = 0.6\beta h_j, & z_1 = 3\beta h_j, \\ z_2 = 2\beta h_j, & z_3 = 1.3\beta h_j, & z_4 = 0.3\beta h_j & \end{array}\right\} \quad (3.48)$$

It is already indicated that the evaluation of the free energy is necessary to ensure that the system is in equilibrium. Hence, the contribution of the free energy to the thermodynamic phase stability has been calculated using Eq. (3.38). Depending on the Hamiltonian of the system mentioned in Eq. (3.37), the partition function written as follows:

$$\begin{aligned} Z &= K_1\cosh(F_1)+K_2\cosh(F_2)+K_3\cosh(F_3)+K_4\cosh(F_4)+K_5\cosh(F_5)+ \\ &\quad K_6\cosh(F_6)+K_7\cosh(F_7)+K_8\cosh(F_8)+K_9\cosh(F_9)+K_{10}\cosh(F_{10}) \\ &\quad +K_{11}\cosh(F_{11})+K_{12}\cosh(F_{12}). \end{aligned} \tag{3.49}$$

where,

$$\begin{aligned} &K_1 = e^{(\frac{15}{4}t+\frac{9}{4}\beta D_A+\frac{25}{4}\beta D_B)}, \quad K_2 = e^{\left[\frac{9}{4}(t+\beta D_A+\beta D_B)\right]}, \quad K_3 = e^{(\frac{3}{4}t+\frac{9}{4}\beta D_A+\frac{1}{4}\beta D_B)} \\ &K_4 = e^{(-\frac{15}{4}t+\frac{9}{4}\beta D_A+\frac{25}{4}\beta D_B)}, \quad K_5 = e^{\left[\frac{9}{4}(-t+\beta D_A+\beta D_B)\right]}, \quad K_6 = e^{(-\frac{3}{4}t+\frac{9}{4}\beta D_A+\frac{1}{4}\beta D_B)} \\ &K_7 = e^{(\frac{5}{4}t+\frac{1}{4}\beta D_A+\frac{25}{4}\beta D_B)}, \quad K_8 = e^{(\frac{3}{4}t+\frac{1}{4}\beta D_A+\frac{9}{4}\beta D_B)}, \quad K_9 = e^{\left[\frac{1}{4}(t+\beta D_A+\beta D_B)\right]} \\ &K_{10} = e^{(-\frac{5}{4}t+\frac{1}{4}\beta D_A+\frac{25}{4}\beta D_B)}, \quad K_{11} = e^{(-\frac{3}{4}t+\frac{1}{4}\beta D_A+\frac{9}{4}\beta D_B)}, \quad K_{12} = e^{\left[\frac{1}{4}(-t+\beta D_A+\beta D_B)\right]} \end{aligned} \tag{3.50}$$

and,

$$\begin{aligned} &F_1 = \frac{3}{2}\beta h_i+\frac{5}{2}\beta h_j, \quad F_2 = \frac{3}{2}\beta(h_i+h_j), \quad F_3 = \frac{3}{2}\beta h_i+\frac{1}{2}\beta h_j, \\ &F_4 = \frac{3}{2}\beta h_i-\frac{5}{2}\beta h_j, \quad F_5 = \frac{3}{2}\beta(h_i-h_j), \quad F_6 = \frac{3}{2}\beta h_i-\frac{1}{2}\beta h_j \\ &F_7 = \frac{1}{2}\beta h_i+\frac{5}{2}\beta h_j, \quad F_8 = \frac{1}{2}\beta h_i+\frac{3}{2}\beta h_j, \quad F_9 = \frac{1}{2}\beta(h_i+h_j), \\ &F_{10} = \frac{1}{2}\beta h_i-\frac{5}{2}\beta h_j, \quad F_{11} = \frac{1}{2}\beta h_i-\frac{3}{2}\beta h_j, \quad F_{12} = \frac{1}{2}\beta(h_i-h_j), \end{aligned} \tag{3.51}$$

CHAPTER FOUR

Results and Discussion

In this chapter, the considered magnetic properties of the mixed-spin Ising systems, were investigated numerically by using the developed Oguchi approximation, in order to clarify the physical background for the characteristic phenomena that observed in the mixed ferrimagnetic models. The effect of a single-ion anisotropy on the compensation phenomenon was taken into consideration. Besides, the effect of the structural lattice on the magnetization curves and the phase diagrams of these systems were shown.

4.1 The Distinction between MFA and OA

First, let us discuss the obtained results by Oguchi method and comparing them with the results obtained by mean-field theory [63]. From Figure 4.1 the magnetization curve of the considered system can be seen at $D_A/|J| = 2.0$ and $D_B/|J| = -0.5$, for z=6, goes more

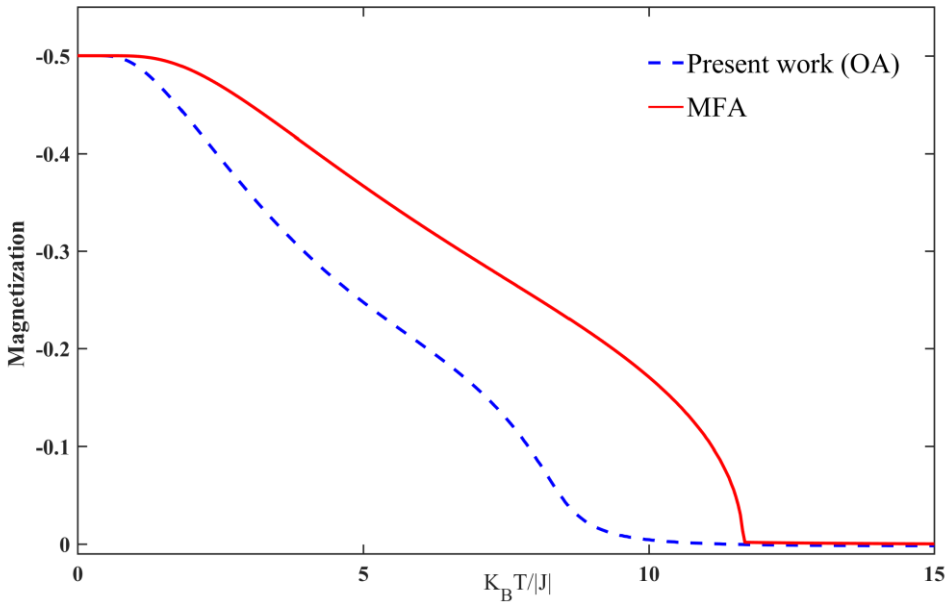

Figure 4.1: The temperature dependences of the total magnetization *m* for the mixed–spin Ising ferrimagnetic system with z=6 (sc), when the values of $D_A/|J| = 2.0$, and$D_B/|J| = -0.5$

rapidly to zero than that of the MFA. This is because of the coupled effect of Oguchi's pair that is correlated to the rest of the lattice with an effective field [65]. One can observe, Figure 4.2, the distinction between the areas of the two curves of the sublattice magnetizations and

the same values of single-Ion anisotropies. The values of Anisotropies were taken depending on the Phase Diagram Shown in Figure 4.3 obtained by Hadey et al.[63].

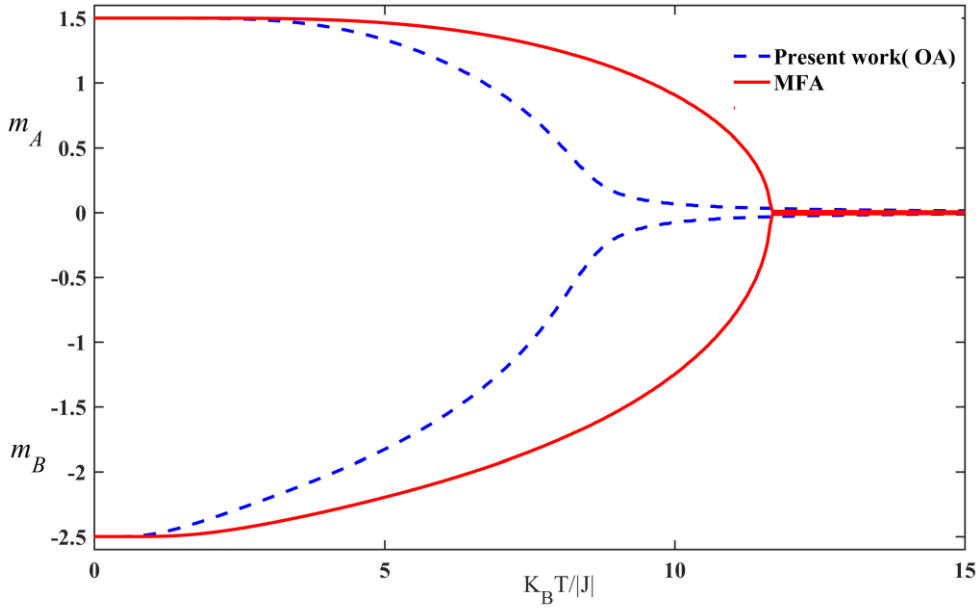

Figure 4.2: The temperature dependences of the sublattice magnetizations m_A, m_B for the mixed–spin Ising ferrimagnetic system with z=6 (sc) when the values of $D_A/|J| = 2.0$, and $D_B/|J| = -0.5$.

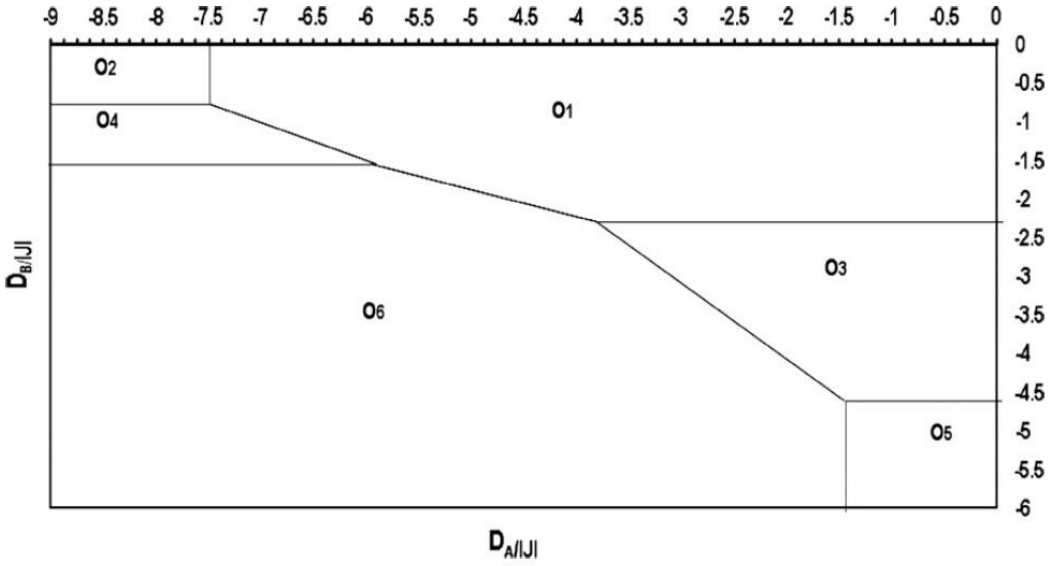

Figure 4.3: Phase Diagram of the mixed spin-3/2 and spin-5/2 Blume-Capel Ising Model for simple cubic lattice [63].

4.2 Critical Behavior of Magnetization

In this section, the critical behavior or Curie temperature (T_C) will be investigated. At this particular temperature, the material undergoes a second order phase transition from the ferrimagnetic phase to the paramagnetic one. The effect of different single-ion anisotropies $D_A/|J|$ and $D_B/|J|$ is shown in Figure 4.4 which studies the total magnetization versus $K_BT/|J|$ for simple cubic lattice at a fixed value of $D_A/|J| = -2.0$ and different values of $D_B/|J|$, whereas for face-centered cubic lattice, the system is at $D_A/|J| = -0.5$ and different values of $D_B/|J|$, respectively.

It is clear that the critical temperature depends substantially on the crystal field where the area under the curve is the ordered phase while above the curve is the disordered phase or paramagnetic phase. Figure 4.5 shows the sublattice magnetizations for the same value of $D_A/|J|$ and different values of $D_B/|J|$ for (z=6) and (z=12). It reveals that the spontaneous magnetization does not vanish directly to zero (as in MFA) instead it decreases gradually. It is similar to the effect as if there is an external field, but since the investigated system is at h=0, so one can conclude that this kind of behavior is due to the effective field [52]. Figure 4.6 and Figure 4.7 show the total and sublattice magnetizations for fixed values of $D_B/|J|$ and different values of $D_A/|J|$ for both lattices. Since $S_j > S_i$, it obvious that the magnetization changes with $D_B/|J|$ more rapidly than with $D_A/|J|$.

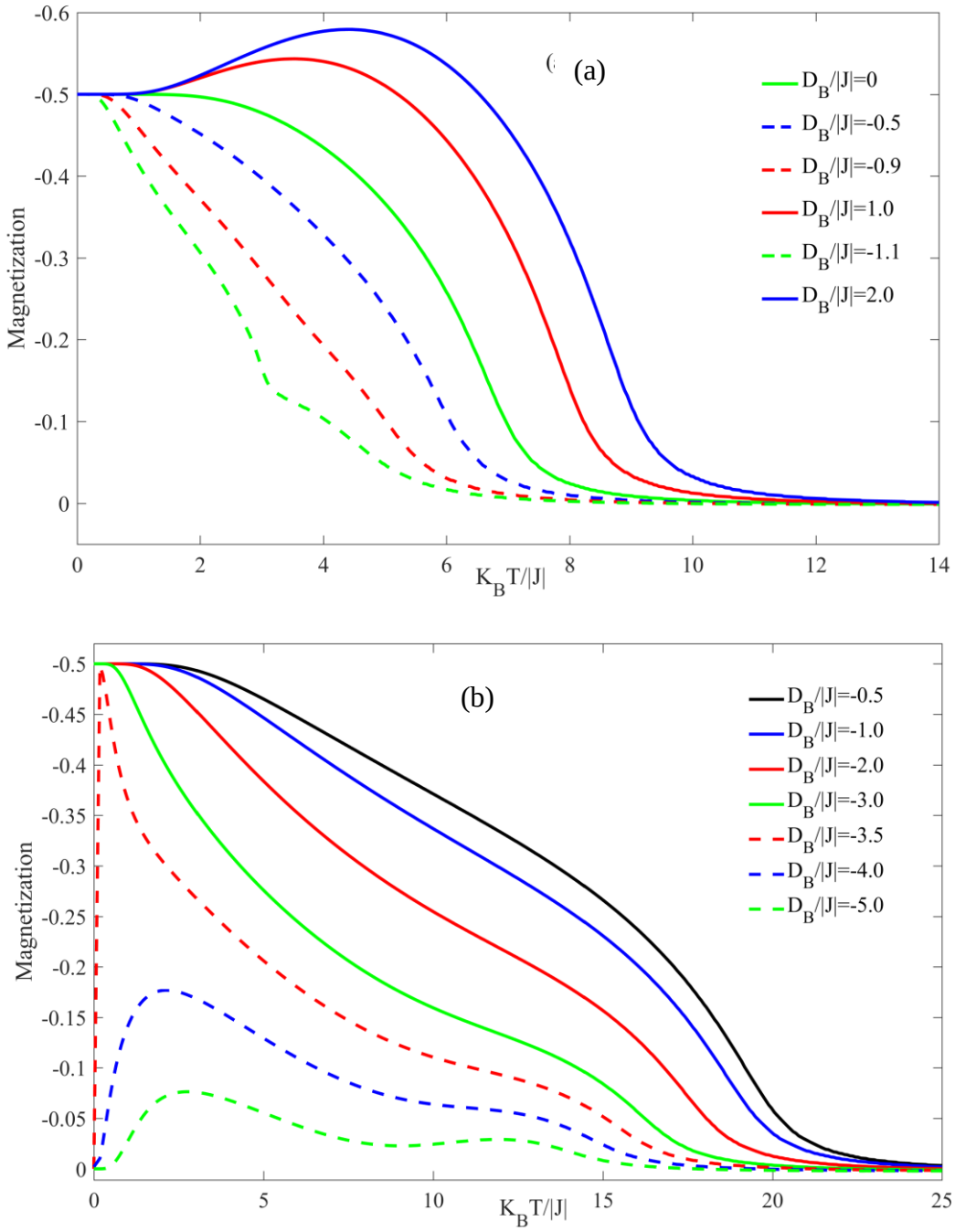

Figure 4.4: Thermal dependence of total magnetization at constant values of $D_A/|J|$and different values of $D_B/|J|$ (a) for z=6 lattice at constant $D_A/|J| = -2.0$ (b) for z=12 lattice at $D_A/|J| = -0.5$.

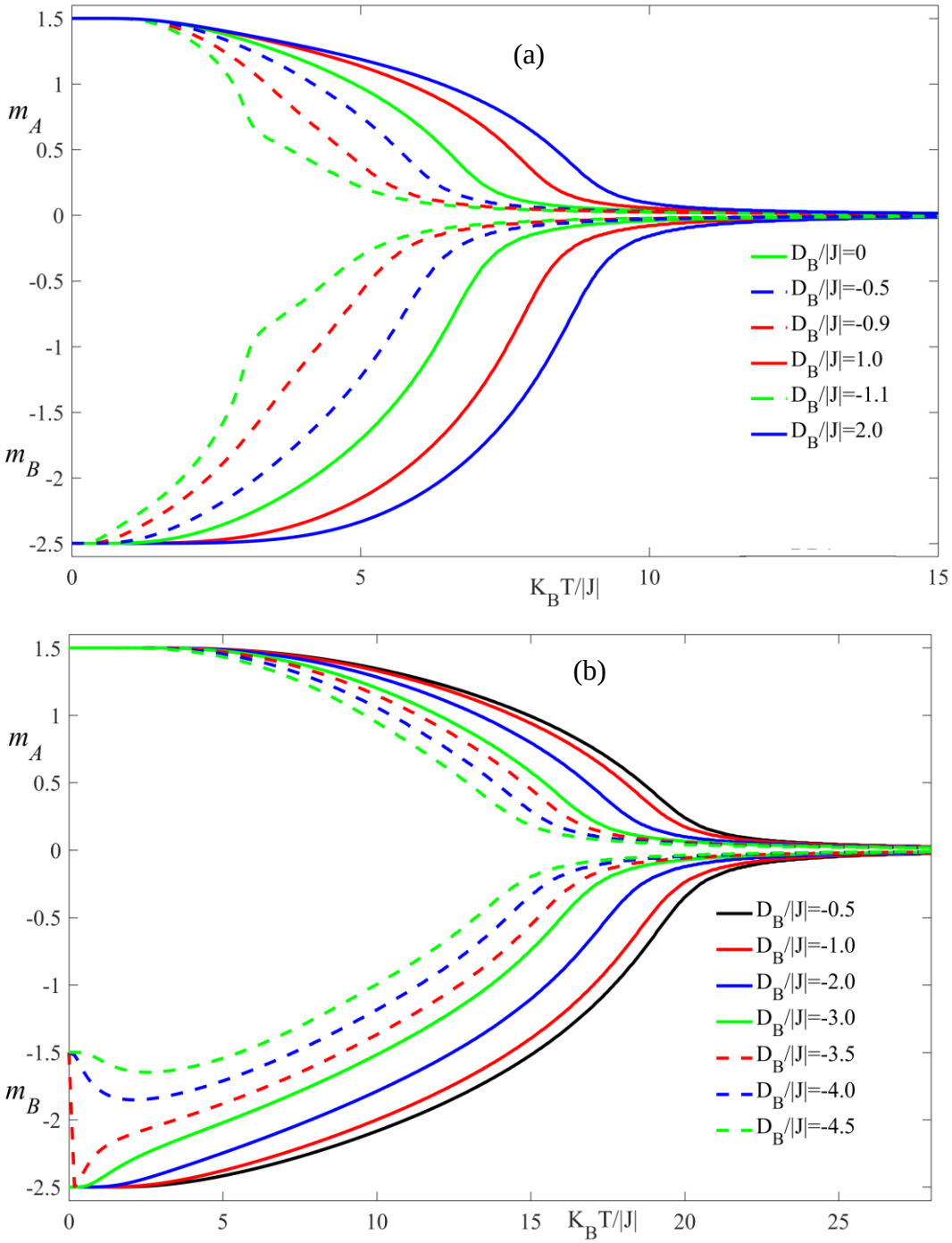

Figure 4.5: Thermal dependence of sublattice magnetizations at constant values of $D_A/|J|$and different values of $D_B/|J|$ (a) for z=6 lattice at constant $D_A/|J| = -2.0$ (b) for z=12 lattice at $D_A/|J| = -0.5$.

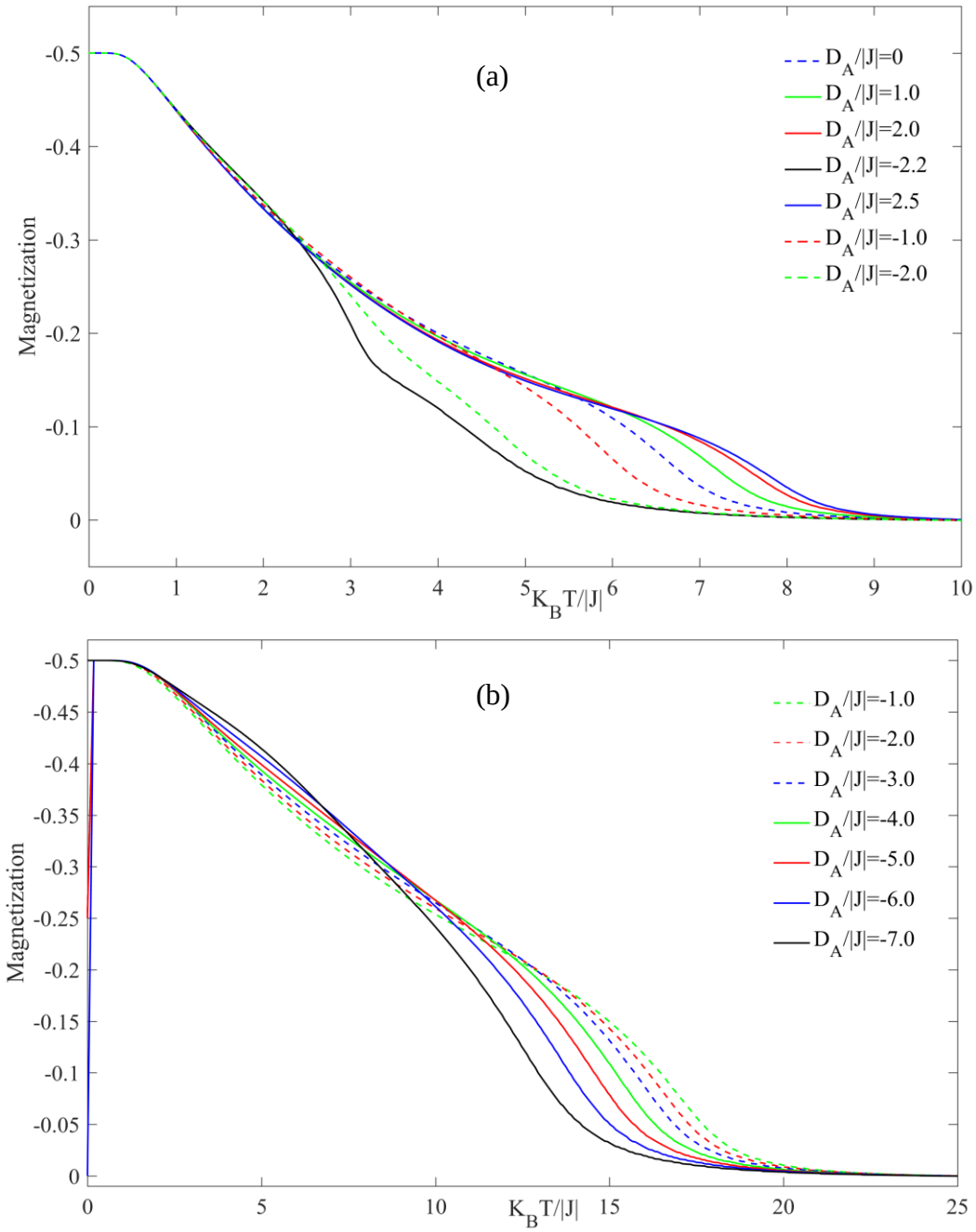

Figure 4.6: Thermal dependence of total magnetization at constant values of $D_B/|J|$and different values of $D_A/|J|$ (a) for z=6 lattice at constant $D_B/|J| = -1.0$ (b) for z=12 lattice at $D_B/|J| = -2.0$.

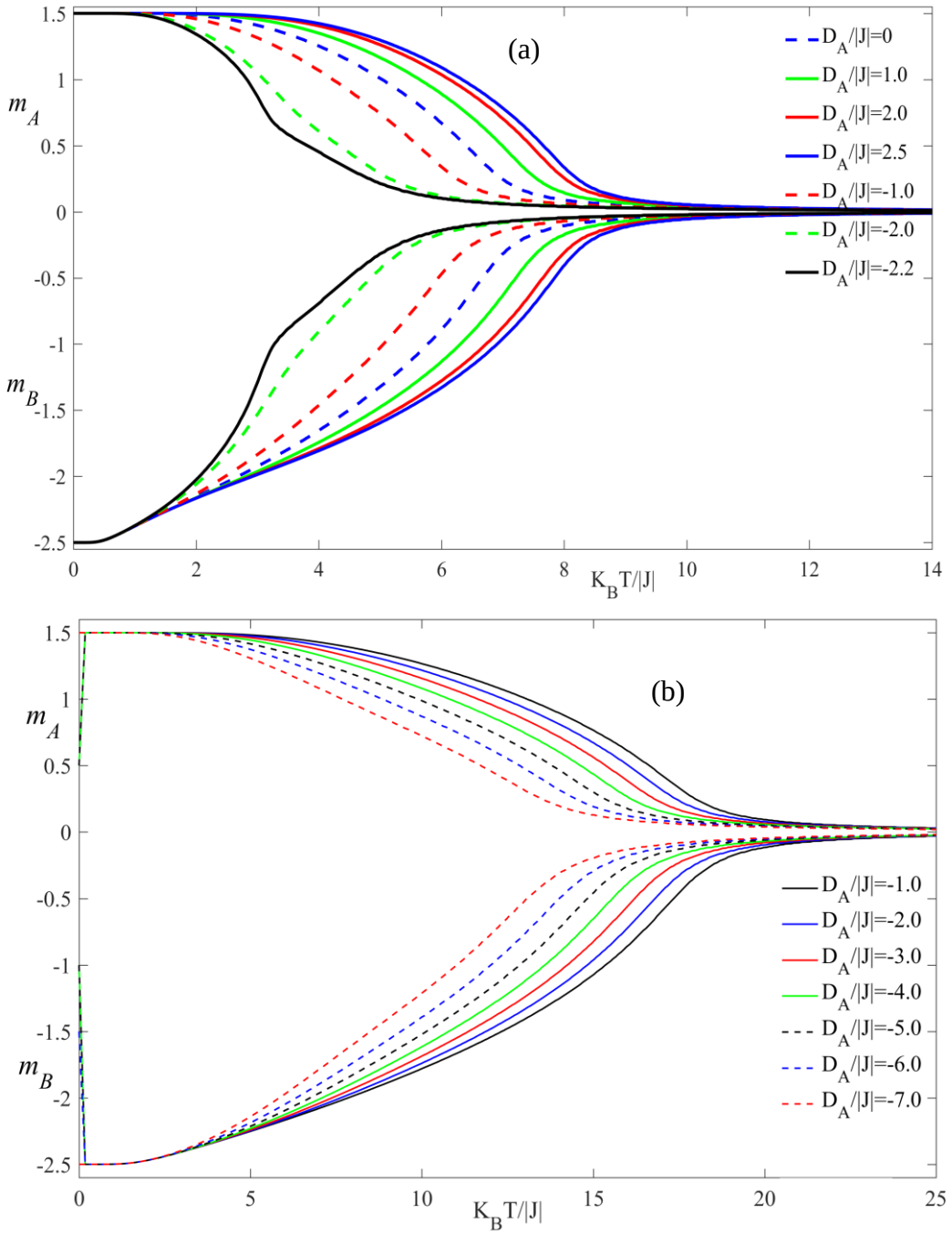

Figure 4.7: Thermal dependence of sublattice magnetization at constant values of $D_B/|J|$and different values of $D_A/|J|$ (a) for z=6 lattice at constant $D_B/|J| = -1.0$ (b) for z=12 lattice at $D_B/|J| = -2.0$

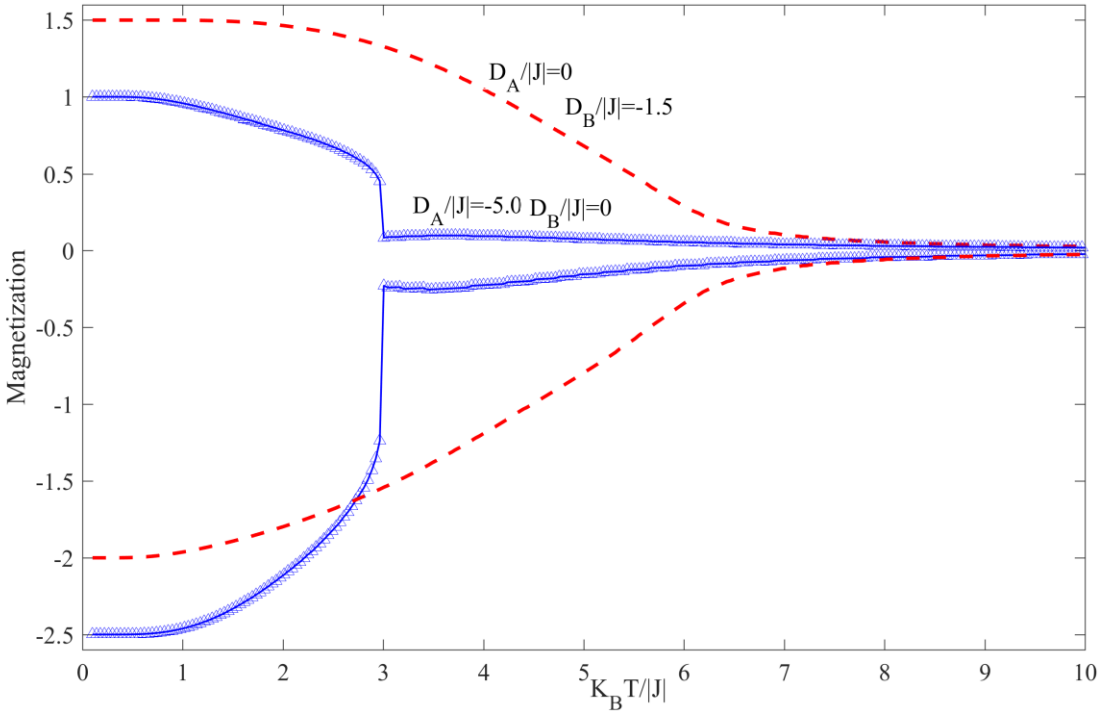

Figure 4.8: Thermal dependence of sublattice magnetizations for different values of anisotropies showing the new phases (1, -5/2) and (3/2, -2) for z=6.

Figure 4.8 stands for the interesting features of the considered system under the influence of certain values for the magnetic anisotropies $D_A/|J|, D_B/|J|$ acting on the sublattice magnetizations of A and B sites, respectively. That is to say, the system experienced new phases for sc lattice which are (1,-5/2) and (3/2,-2) for the values of $D_A/|J|$=-5.0, $D_B/|J|$=0 and $D_A/|J|$=0, $D_B/|J|$=-1.5, respectively.

4.3 The Compensation Behavior

In this section, some compensation behaviors for both structural lattices sc (z=6) and fcc (z=12), are presented respectively. Then the influence of ion-anisotropy parameters on the appearance and magnitude of compensation temperatures(T_K) is discussed. On observing

Figure 4.9, it reveal interesting phenomena regards compensation temperatures for both lattices at $D_B/|J| = -1.92$ for (z=6) and $D_B/|J| = -5.0$ for (z=12).

Figures 4.9 (a) and (b) show a multicompensation behavior for different values of $D_A/|J| = 0, 1.0, 2.0$ for (z=6) and $D_A/|J| = -2.0, -2.5, -3.0$ for (z=12) while Figures 4.9 (c) and (d) depicts the act of absolute values of sublattice magnetizations m_A and m_B at $D_A/|J| = 1.0$ and $D_A/|J| = -3.0$ for sc and fcc structures, respectively. It is worth to note that the compensation points are induced by the presence of magnetic anisotropy for the atom B, which is possible only in the ferromagnetic phase. These sublattice magnetizations undergo a cancelation but it is still incomplete so there a residual spontaneous magnetization in the system ($M \neq 0$). This is evidence to the antiferromagnetic nearest neighbor interactions [35]. This interaction tends to align neighboring spins in opposite directions as the system's temperature is increased, so the direction of this residual magnetization can switch due to the thermal agitation.

It is noticeable to see that the magnitude of spontaneous magnetization between $T_K - T_K$ is larger than that between $T_K - T_C$ since as T approaches T_C more and more magnetic spins will be oriented randomly giving smaller spontaneous magnetization [37]. The circles are

shown in Figure 4.9 (c) and (d) indicate the crossing points between the absolute magnitudes of $|m_A|$ and $|m_B|$, which prove the eligibility of Eqs. (3.45) and (3.48).

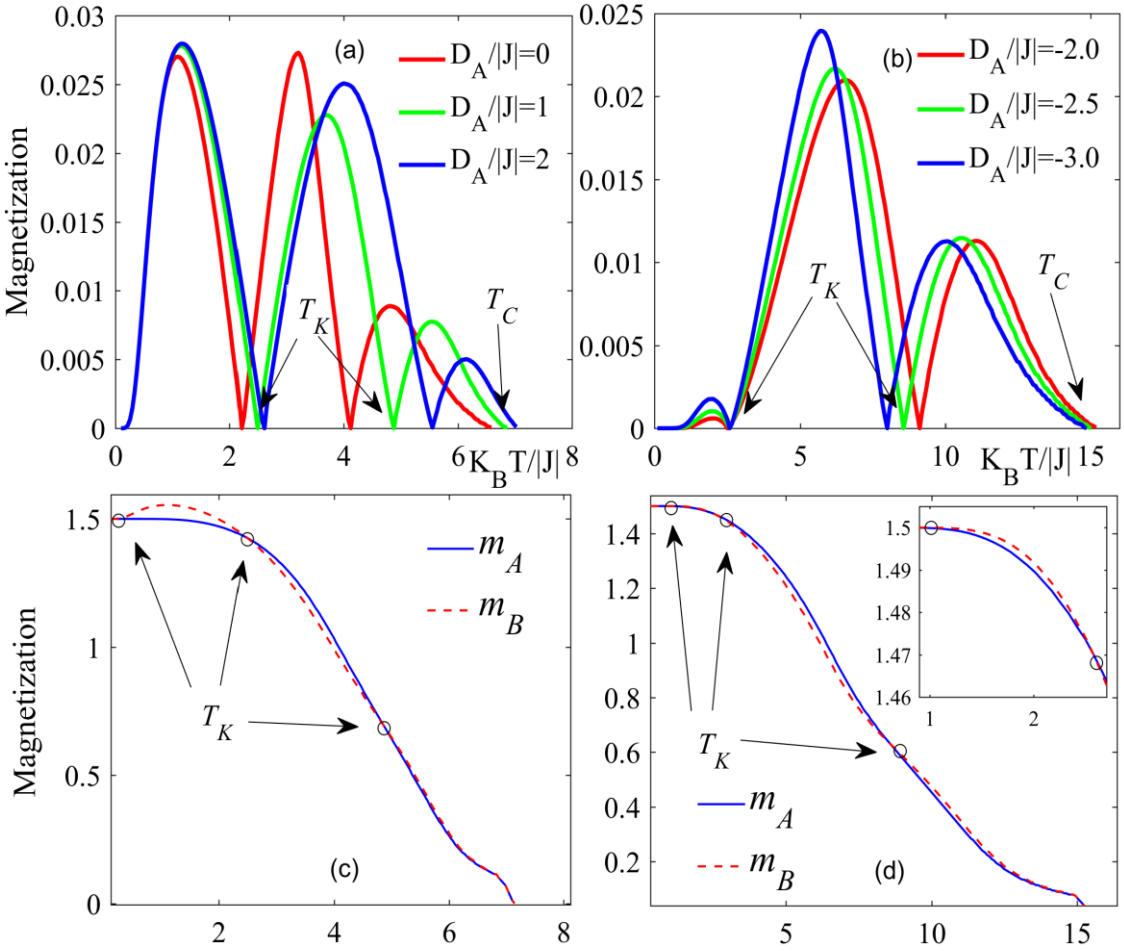

Figure 4.9: (a) Temperature dependence of the total magnetization of z=6 for $D_B/|J| = -1.92$and different values of $D_A/|J|$. (b) Temperature dependence of the total magnetization of z=12 for $D_B/|J| = -5.0$ and several values of $D_A/|J|$. (c) Temperature dependence of $|m_A|$ and $|m_B|$ at z=6 for $D_A/|J| = 1.0$ and $D_B/|J| = -1.92$. (d) $|m_A|$ and $|m_B|$ at z=12 for $D_A/|J| = -3.0$ and $D_B/|J| = -5.0$.

From the previous results, it is clear that the appearance of compensation points is independent of $D_A/|J|$, and this prediction is similar to that obtained by Reyes at al. [68] i.e. $D_B/|J|$ plays a relevant role in the appearance of the compensation phenomena, while $D_A/|J|$induces the location of the compensation points. In other words, our results are in a good agreement with ones obtained by Reyes et al. [68]. However, the system revealed three compensation points, whilst Reyes et al. study shows two compensation temperatures only

i.e. the developed model has given a clear impression about the investigated system compared to the method that has been used by Reyes et al. [68]. Therefore, the relation between T_K and $D_A/|J|$ can be represented in the plane $(D_A/|J|, K_B T/J)$ as shown in Figure 4.10, for a fixed value of $D_B/|J| = -2.8$. At negative values of $D_A/|J|$, T_K has taken the value (1.6124 k) at $D_A/|J| \geq 0, and\ T_K$ starts to increase linearly which is in a good agreement with the results obtained by Reyes et al. [68] for the same system considered but the authors have used Monte Carlo simulation under the influence of different values of $D_B/|J|$.

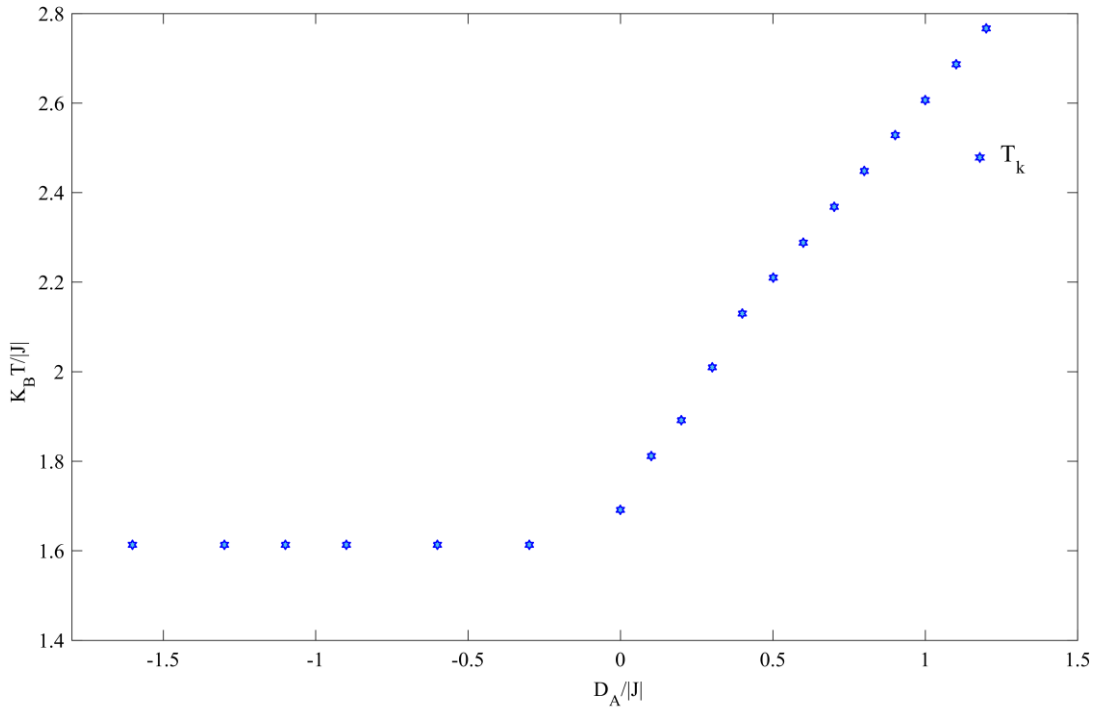

Figure 4.10: Magnetic anisotropy dependence of the compensation temperature for the mixed-spin Ising ferrimagnet with the coordination number z=6, when the value of $D_A/|J|$ is changed, with a constant value of $D_B/|J| = -2.8$.

4.4 Free Energy of the System

The free energy of the system under study was calculated numerically by using Eq. (3.38) for sc and fcc lattices, respectively. Figure 4.11 shows the free energy of the system with a fixed value of $D_A/|J|$ and various values of $D_B/|J|$. Figure 4.12 illustrates the free energy for constant value of $D_B/|J|$ and different values of $D_A/|J|$, respectively.

It can be seen that it shows an inflexion that corresponds a discontinuous behavior and at a critical temperature, the free energy of the system is continuous. Results shown in Figures. 4.11b and 4.12b are consistence with those derived from Figures 4.5b and 4.7b. On the other hand it can be seen that the system which is considered to behave as second order phase transition, one can compare the sublattice magnetization curves shown in Figures 4.5a and 4.7a with those depicted in Figures 4.11a and 4.12a [69].

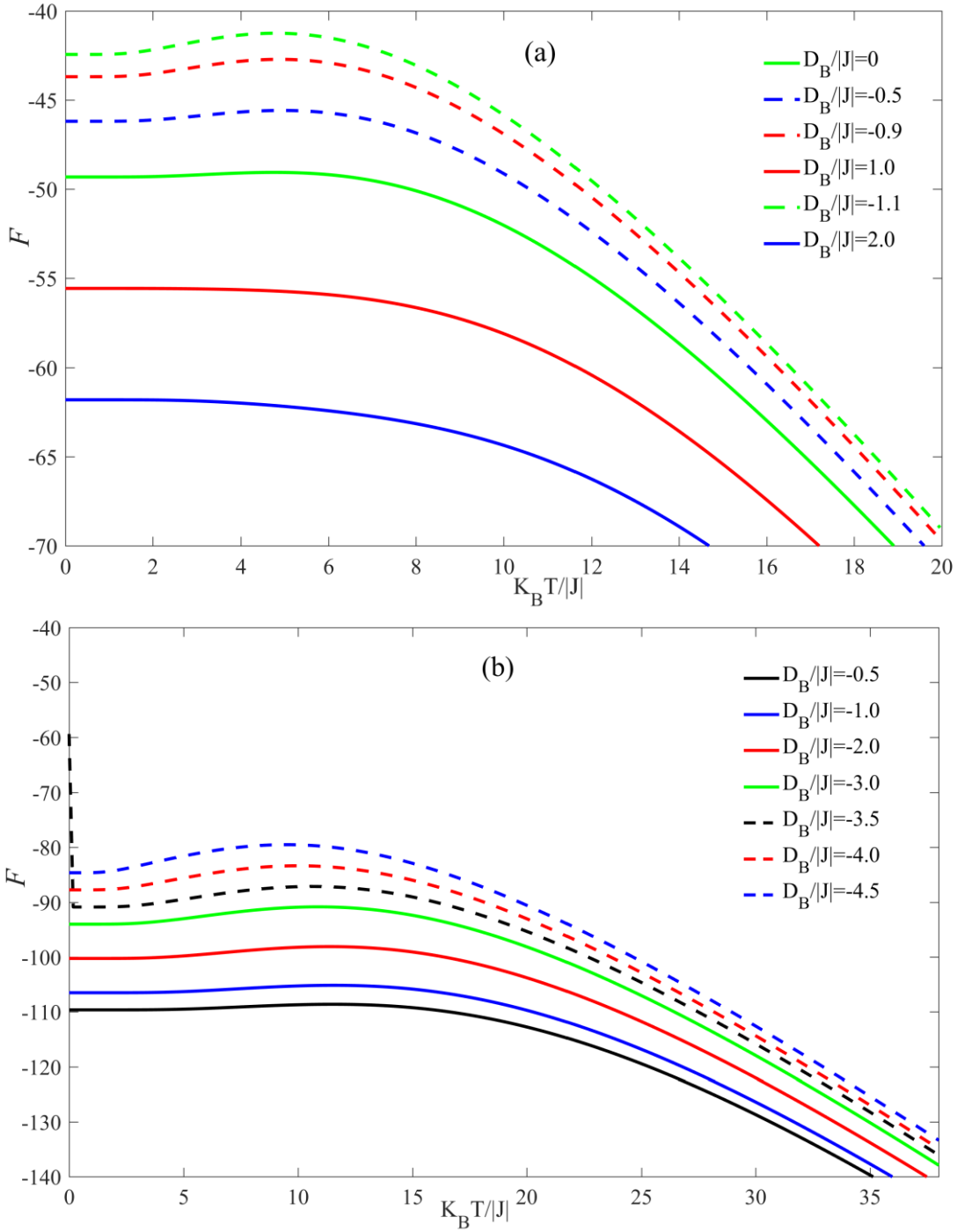

Figure 4.11: Free energy of the system for (a) Simple-Cubic lattice at $D_A/|J| = -2.0$ and different values of $D_B/|J|$. (b) Face-Centered Cubic lattice at $D_A/|J| = -0.5$ and various values of $D_B/|J|$.

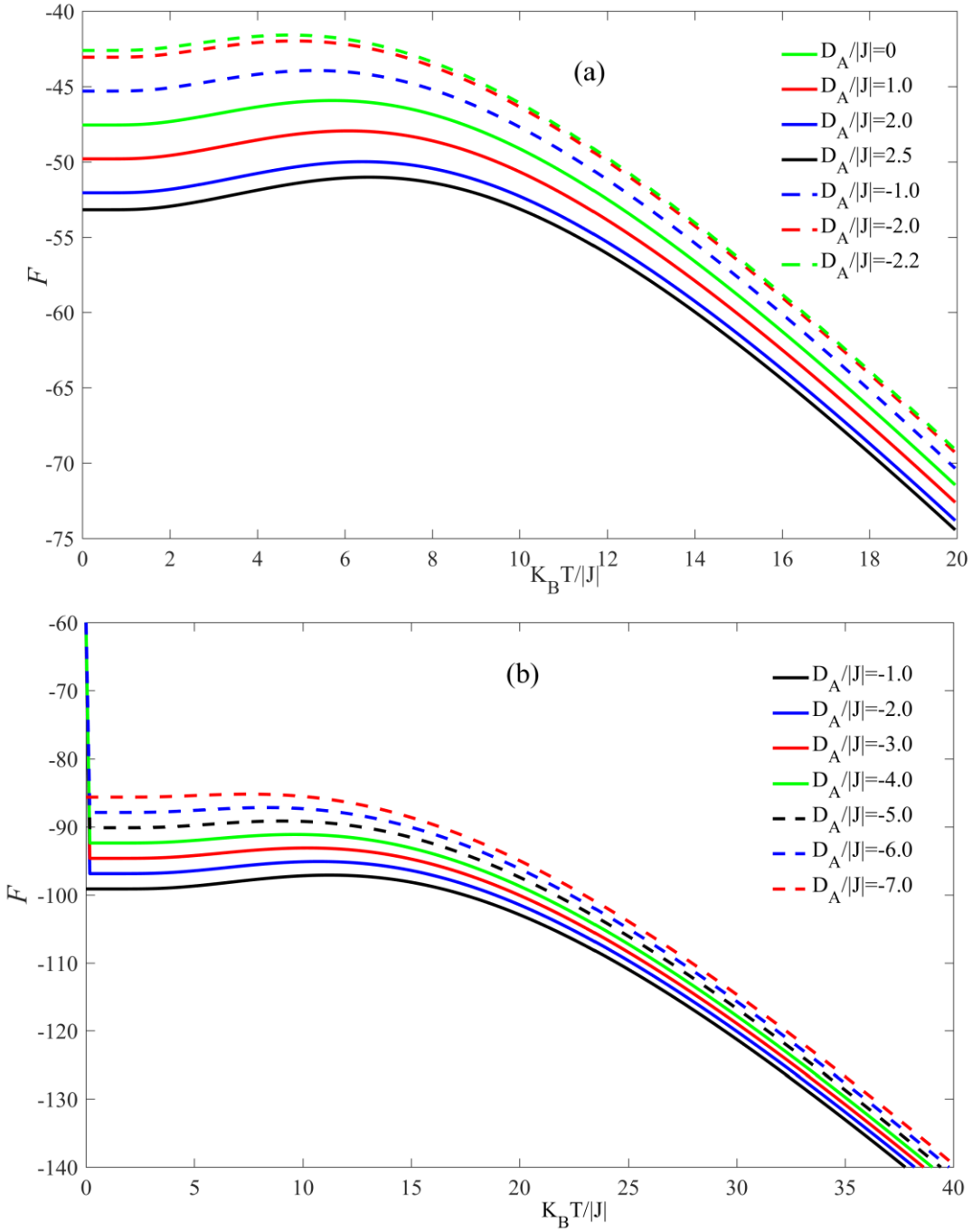

Figure 4.12: Free energy of the system for (a) Simple-Cubic lattice at $D_B/|J| = -1.0$ and different values of $D_A/|J|$. (b) Face-Centered Cubic lattice at $D_B/|J| = -2.0$ and various values of $D_A/|J|$.

4.5 Types of Behaviors

Certain types of behaviors were obtained for magnetization of particular values of $D_A/|J|$ and $D_B/|J|$, which were first introduced by Neél in 1948 [70].

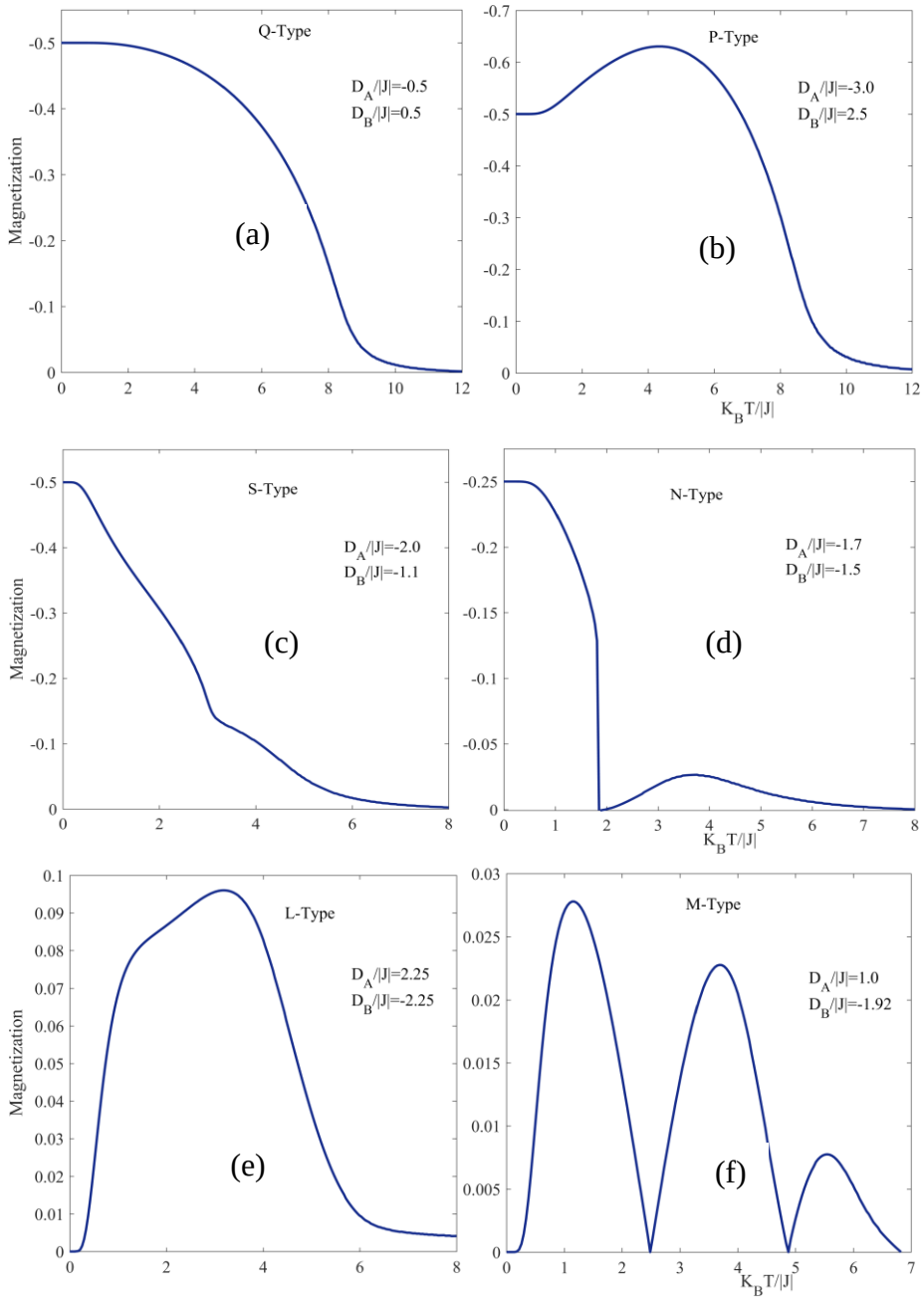

Figure 4.13: Different types of thermal dependence of magnetizations for z=6. (a) Q-type for $D_A/|J|$=-0.5 and $D_B/|J|$=0.5 (b) P-type for $D_A/|J|$= -3.0 and $D_B/|J|$= 2.5 (c) S-type for $D_A/|J|$=-2.0 and $D_B/|J|$=-1.1 (d) N-type for $D_A/|J|$=-1.7 and $D_B/|J|$=-1.5 (e) L-type for $D_A/|J|$=2.25 and $D_B/|J|$=-2.25 (f) M-type for $D_A/|J|$=1.0 and $D_B/|J|$=-1.92.

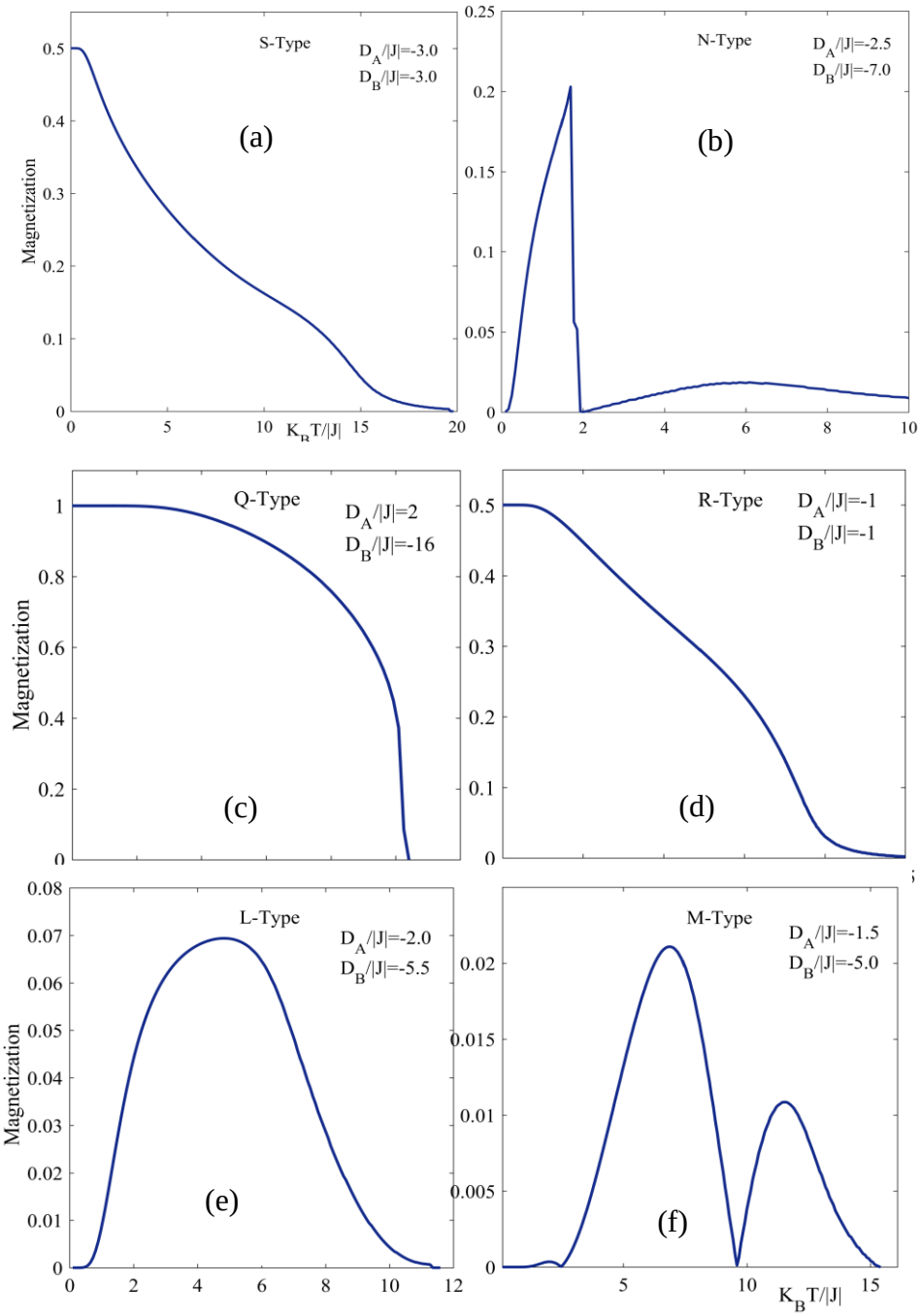

Figure 4.14: Different types of thermal dependence of magnetizations for z=12. (a) S-type for $D_A/|J|$=-3.0 and $D_B/|J|$= -3.0 (b) N-type for $D_A/|J|$= -2.5 and $D_B/|J|$= -7.0 (c) Q-type for $D_A/|J|$= 2 and $D_B/|J|$= -16 (d) R-type for $D_A/|J|$= -1.0 and $D_B/|J|$= -1.0 (e) L-type for $D_A/|J|$=-2.0 and $D_B/|J|$= -5.5 (f) M-type for $D_A/|J|$= -1.5 and $D_B/|J|$= -5.0.

The considered system can reveal many types of typical thermal dependence of magnetization and for both lattices usually present in the crystallized ferrimagnetic alloys [28]. Six of the results for the sc and fcc lattices are depicted in Figure 4.13 and Figure 4.14 where the thermal behavior of magnetizations are shown for different values of anisotropies.

As seen from the figures, the system exhibit Q-type behavior at $D_A/|J| = -0.5$, $D_B/|J| = 0.5$ and $D_A/|J| = 2.0$, $D_B/|J| = -16.0$ for sc and fcc lattices, respectively. On the other hand the N curves exhibit a compensation point at $D_A/|J| = -1.5$, $D_B/|J| = -1.7$ and $D_A/|J| = -2.5$, $D_B/|J| = -7.0$ for sc and fcc lattices, respectively, which is classified after Neél as the N-type. It can be seen for both lattice structures, that they have almost the same behavior types at different values of anisotropies, which are S-, P-, L-, M-, for sc lattice and S-, R-, L-, M-type for fcc lattice.

CHAPTER FIVE

Conclusions and Future Studies

CHAPTER FIVE CONCLUSIONS AND FUTURE STUDIES

5.1 Conclusions

It can be seen that within reviewing the results of the mixed spin 3/2 and spin 5/2 ferrimagnetic Ising system by using the developed Oguchi approximation:

1- The considered system shows multicompensation points in the low range of temperatures. However, the system; at the same time shows transition temperatures (Curie Temperatures) in the moderate ranges of $(14\text{-}25)k$ for fcc lattice and of $(6\text{-}11)k$ for sc lattice, respectively.

2- Curie temperatures are slightly effected when changing the magnetic anisotropy for sublattice of atoms A in the ranges $2.5 \geq D_A/|J| \geq -2.2$ for sc lattice and $-1.0 \geq D_B/|J| \geq -7.0$ for fcc lattice. However, Curie temperature are clearly effected by increasing the coordination number (z) that it can reach about $(25k)$ for the fcc lattice.

3- Single compensation temperatures were noticed when the magnetic anisotropy is $D_B/|J| = -2.8$ for the simple cubic lattice only.

4- Three compensation temperatures were noticed when the magnetic anisotropy is in the ranges $-1.99 \leq D_B/|J| \leq -1.85$ and $-5.2 \leq D_B/|J| \leq -4.8$ for sc and fcc lattices, respectively, with various values of magnetic anisotropy for sublattices of atoms A.

5- It was found that the system experiences the first and second order phase transitions, however the second order phase transition is the dominant one in revealing the properties of the system in the planes $(m_A, K_BT/|J|)$ $(m_B, K_BT/|J|)$, as shown in Figure 4.5 and Figure 4.7, respectively. These phases can be recognized, which appear in our system within studying the behaviors in the plane $(F, K_BT/|J|)$ for both structural lattices depicted in Figure 4.11 and Figure 4.12, respectively.

6- New phases for the considered system have been obtained, namely (3/2, -2), and (1, -5/2) for appropriate values of anisotropies ($D_A/|J|$=0, $D_B/|J|$=-1.5) and ($D_A/|J|$=-5.0, $D_B/|J|$=0), respectively as shown in Figure 4.8.

7- The system responded for induction of multicompensation temperatures at certain values of magnetic anisotropies (i.e. Crystal Fields) in a range of ($D_A/|J|$)at fixed values of $D_B/|J|$, but out of these ranges, one can observe that the system has no response.

8- It is noted that the results concerning the multiplicity of compensation temperatures are better than the results obtained by Hadey K. using Mean field approximation (MFA) [63].

9- The importance of compensation points resembled by the fact that at this particular point, only a small driven field is required to reverse the direction of magnetization in the hysteresis loop hence giving a material with small hysteresis loop and less energy losses [45].

5.2 Future Studies

1- A theoretical study of the magnetic hysteresis loop of the mixed spin-3/2 and spin-5/2 Blume-Capel Ising model in the presence of an oscillating magnetic field.

2- A study of Blume-Capel Ising model with different single-ion anisotropies by using the effective filed theory.

3- A study of the Thermodynamic functions of the considered system such as internal energy, heat capacity, entropy and magnetic susceptibility.

4. The study of a decorated mixed spin-3/2 and spin-5/2 Ferrimagnetic Blume-Capel Ising models, with different single-ion anisotropies.

REFERENCES

REFERENCES

[1] C. Heck, Magnetic Materials and their Applications, pp. 686–753, 1974.

[2] P. Fuley, J. Lee, Electronic, Magnetic and Optical Materials, 2nd Ed., CRC Press, 2017.

[3] J. S. Miller and M. Drillon, Magnetism: Molecules to materials IV, John Wiley & Sons, 2006.

[4] H. N. Russell and F. A. Saunders, New regularities in the spectra of the alkaline earths, Astrophys. J., vol. 61, pp. 38–61, 1925.

[5] W. Callister and D. Rethwisch, Materials science and engineering: an introduction, 7th Ed., John Wiley & Sons, 2007.

[6] J. M. D. Coey, Magnetism and magnetic materials, Cambridge University Press, 2010.

[7] J. P. Schaffer, A. Saxena, S. D. Antolovich, T. H. Sanders, and S. B. Warner, The science and design of engineering materials, Irwin Chicago, 1995.

[8] D. Jiles, Introduction to Magnetism and Magnetic Materials, Chapman and Hall, 1991.

[9] B.D. Cullity, C. D. Graham, Introduction to Magnetic Materials, 2nd Ed., John Wiley & Sons, 2009.

[10] N. A. Spaldin and J. Mansbridge, Magnetic materials: fundamentals and applications, 2nd Ed., Cambridge University Press, 2010.

[11] K. J. Klabunde, Nanoscale Materials in Chemistry, John Wiley & Sons, 2001.

[12] P. S. Aithal, and H. J. Ravindra, Textbook of Engineering Physics, ACME Learning Private Limited, 2011.

[13] C. Pickover, Archimedes to Hawking: Laws of Science and the Great Minds Behind Them, Oxford University Press, 2008.

[14] R. A. McCurrie, Ferromagnetic Materials Structure and Properties, Academic Press Limited, 1994.

[15] S. Chikazumi, Physics of Ferromagnetism, 2nd Ed., Oxford University Press, 1997.

[16] C. B. Carter and M. G. Norton, Ceramic materials: science and engineering, Springer Science & Business Media, 2007.

[17] C. P. Poole Jr, Encyclopedic dictionary of condensed matter physics, Academic Press, 2004.

REFERENCES

[18] C. D. Stanciu, A. V. Kimel, F. Hansteen, A. Tsukamoto, A. Itoh, A. Kirilyuk, Th. Rasing, Ultrafast spin dynamics across compensation points in ferrimagnetic GdFeCo: The role of angular momentum compensation, Phys. Rev. B - Condens. Matter Mater. Phys., vol. 73, no. 22, pp. 1–4, 2006.

[19] M. Keskin and M. Ertaş, Existence of a dynamic compensation temperature of a mixed spin-2 and spin-5/2 Ising ferrimagnetic system in an oscillating field, Phys. Rev. E, vol. 80, no. 6, p. 61140, 2009.

[20] E. Ising, Beitrag zur Theorie des Ferromagnetismus, Zeitschrift fur Phys., vol. 31, no. 1, pp. 253–258, 1925.

[21] R. Peierls and M. Born, On Ising's model of ferromagnetism, Math. Proc. Cambridge Philos. Soc., vol. 32, no. 3, p. 477, 1936.

[22] Y. Nakamura, Existence of a compensation temperature of a mixed spin-2 and spin-5/2 Ising ferrimagnetic system on a layered honeycomb lattice, Phys. Rev. B - Condens. Matter Mater. Phys., vol. 62, no. 17, pp. 11742–11746, 2000.

[23] T. Oguchi and Y. Obata, A Theory of Antiferromagnetism, Prog. Theor. Phys., vol. 9, no. 4, pp. 359–369, 1953.

[24] T. Oguchi, A theory of antiferromagnetism, II, Prog. Theor. Phys., vol. 13, no. 2, pp. 148–159, 1955.

[25] B. R. Cooper, Sublattice magnetization and resonance frequency of antiferromagnets with large uniaxial anisotropy, Phys. Rev., vol. 120, no. 4, pp. 1171–1175, 1960.

[26] T. Ishikawa and T. Oguchi, Critical Behavior of the Spin System with Anisotropic Exchange Interactions. II. Two Dimensional lattice, J. Phys. Soc. Japan, vol. 31, no. 4, pp. 1021–1025, 1971.

[27] F. Y. Wu, Phase Diagram of a Spin-One Ising System, Chinese J. Phys., vol. 16, no. 2, pp. 153–156, 1978.

[28] T. Kaneyoshi, E. F. Sarmento, and I. P. Fittipaldi, A compensation temperature induced by transverse fields in a mixed Ising ferrimagnetic system, Jpn. J. Appl. Phys., vol. 27, no. 4, 1988.

[29] T. Kaneyoshi, J. W. Tucker, and M. Jaščur, Differential operator technique for higher spin problems, Phys. A Stat. Mech. its Appl., vol. 186, no. 3–4, pp. 495–512, 1992.

[30] M. Jaščur and T. Kaneyoshi, The effect of anisotropies on the transition temperature in a spin-12 and spin-32 bilayer system with disordered interfaces, Phys. A Stat. Mech. its

Appl., vol. 220, no. 3–4, pp. 542–551, 1995.

[31] A. Bobak and M. Jurčišin, Ferrimagnetism in diluted mixed-spin two-dimensional Ising models, J. Magn. Magn. Mater., vol. 163, no. 3, pp. 292–298, 1996.

[32] A. Bobák and M. Jurčišin, "A theoretical study of the diluted mixed spin-1 and spin-3/2 Ising ferrimagnet," Phys. B Condens. Matter, vol. 233, no. 2–3, pp. 187–195, 1997.

[33] M. Jaščur, Exact results for a decorated Ising model, Phys. A Stat. Mech. its Appl., vol. 252, no. 1–2, pp. 217–224, 1998.

[34] A. Bakchich and M. El Bouziani, The semi-infinite spin-3/2 Blume-Capel model, J. Phys. Condens. Matter, vol. 11, no. 32, p. 6147, 1999.

[35] A. Dakhama and N. Benayad, On the existence of compensation temperature in 2d mixed-spin Ising ferrimagnets: an exactly solvable model, J. Magn. Magn. Mater., vol. 213, no. 1, pp. 117–125, 2000.

[36] Y. Nakamura, S. Shin, and T. Kaneyoshi, The effects of transverse field on the magnetic properties in a diluted mixed spin-2 and spin-5/2 Ising system, Phys. B Condens. Matter, vol. 284–288, pp. 1479–1480, 2000.

[37] O.F. Abubrig, D. Horváth, A. Bobák, M. Jaščur, Mean-Field solution of the mixed spin-1 and 2 Ising system with di erent single-ion anisotropies, Physica A, vol. 296, pp. 437–450, 2001.

[38] W. Jiang, G. Wei, and Z. Zhang, Tricritical behavior and magnetic properties for a mixed spin-1 and spin-3/2 transverse Ising model with a crystal field, Phys. Rev. B, vol. 68, no. 13, p. 134432, 2003.

[39] G. S. Tian and H. Q. Lin, Phase transition and ferrimagnetic long-range order in the mixed-spin Heisenberg model with single-ion anisotropy, Phys. Rev. B, vol. 70, no. 10, p. 104412, 2004.

[40] E. Albayrak and A. Yigit, Mixed spin-3/2 and spin-5/2 Ising system on the Bethe lattice, Phys. Lett. A, vol. 353, no. 2–3, pp. 121–129, 2006.

[41] J. Oitmaa and I. G. Enting, A series study of a mixed-spin ferrimagnetic Ising model, J. Phys. Condens. Matter, vol. 18, no. 48, pp. 10931–10942, 2006.

[42] A. Benyoussef, A. El Kenz, and M. El Yadari, Mean field study of decorated ferrimagnetic Ising model, vol. 8, no. 1, pp. 72–77, 2007.

[43] A. Bobák and V. Pokorný and J. Dely, Anomalous behaviour of the magnetic

susceptibility of the mixed spin-1 and spin-½ anisotropic Heisenberg model in the Oguchi approximation, J. Phys. Conf. Ser., vol. 200, no. 2, p. 22001, 2010.

[44] B. Deviren and M. Keskin, Dynamic phase transitions and compensation temperatures in a mixed spin-3/2 and spin-5/2 Ising system, J. Stat. Phys., vol. 140, no. 5, pp. 934–947, 2010.

[45] N. De La Espriella and G. M. Buendía, Magnetic behavior of a mixed Ising 3/2 and 5/2 spin model, J. Phys. Condens. Matter, vol. 23, no. 17, p. 176003, 2011.

[46] J. S. Da Cruz Filho, M. Godoy, and A. S. De Arruda, Phase diagram of the mixed spin-2 and spin-5/2 Ising system with two different single-ion anisotropies, Phys. A Stat. Mech. its Appl., vol. 392, no. 24, pp. 6247–6254, 2013.

[47] G. Mert, The thermodynamic properties of a spin-1/2 Heisenberg ferromagnetic system using Oguchi's method, J. Magn. Magn. Mater., vol. 394, pp. 126–129, 2015.

[48] X. Shi, L. Wang, J. Zhao, and X. Xu,"Dynamic phase diagrams and compensation behaviors in molecular-based ferrimagnet, J. Magn. Magn. Mater., vol. 410, pp. 181–186, 2016.

[49] J. D. Alzate-Cardona, D. Sabogal-Suárez, and E. Restrepo-Parra, Critical and compensation behavior of a mixed spin-3/2 and spin-5/2 Ising ferrimagnetic system in a graphene layer, J. Magn. Magn. Mater., vol. 429, no. September 2016, pp. 34–39, 2017.

[50] M. Ertaş and A. Yılmaz, Dynamic magnetic properties of mixed half-integer ($\sigma = 3/2$) and half-integer ($S = 5/2$) spins: Dynamic effectice-field theory, Comput. Condens. Matter, vol. 14, no. December 2017, pp. 1–7, 2018.

[51] J. R. V Pereira, T. M. Tunes, A. S. de Arruda, and M. Godoy, Thermal properties of the mixed spin-1 and spin-3/2 Ising ferrimagnetic system with two different random single-ion anisotropies, Phys. A Stat. Mech. its Appl., vol. 500, pp. 265–272, 2018.

[52] J. M. Yeomans, Statistical Mechanics of Phase Transitions, Oxford University Press, 1992.

[53] J. Stöhr, H. C. Siegmann, Magnetism From Fundamentals to Nanoscale Dynamics, Springer-Verlag, p. 820, 2006.

[54] T. Bahlagui, H. Bouda, A. El Kenz, L. Bahmad, and A. Benyoussef, Monte Carlo simulation of compensation behavior for a mixed spin-5/2 and spin-7/2 Ising system with crystal field interaction, Superlattices Microstruct., vol. 110, pp. 90–97, 2017.

[55] K. Huang, Statistical Mechanics, 2nd Ed., John Wiley & Sons, 1987.

[56] H. K. Mohamad, Mean-Field Approximation of the Mixed Ferrimagnetic Ising Systems, Scholars' Press, Germany, PhD. Dissertation, 2013.

[57] G. M. Bell and D. A. Lavis, Statistical Mechanics of Lattice Systems, volume II. Springer-Verlag, 1999.

[58] L. Onsager, Crystal statistics. I. A two-dimensional model with an order-disorder transition, Phys. Rev., vol. 65, no. 3–4, pp. 117–149, 1944.

[59] M. Blume, Theory of the First-Order Magnetic Phase Change in UO2, Phys. Rev., vol. 141, no. 2, p. 517, 1966.

[60] M. Kaufman and M. Kanner, Random-field Blume-Capel model: Mean-field theory, Phys. Rev. B, vol. 42, no. 4, pp. 2378–2382, Aug. 1990.

[61] T. Kaneyoshi, Differential Operator Technique, ACTA PHYSICA POŁONICA A vol. 83, no. 6, pp. 703–738, 1993.

[62] H. H. Chen and F. Lee, Constant-coupling approximation of the exchange-interaction model of ferromagnetism, Phys. Rev. B, vol. 48, no. 13, pp. 9456–9461, 1993.

[63] H. K. Mohamad, Spin compensation temperatures induced by longitudinal fields in a mixed spin-3/2 and spin-5/2 Ising ferrimagnet, J. Magn. Magn. Mater., vol. 323, no. 1, pp. 61–66, 2011.

[64] A. Bobák, V. Pokorný, and J. Dely, Critical properties of the mixed spin-1 and spin-1/2 anisotropic Heisenberg model in the Oguchi approximation, Phys. A Stat. Mech. its Appl., vol. 388, no. 11, pp. 2157–2167, 2009.

[65] J. Dely, J. Strečka, and L. Canova, Phase Diagram of the Spin-1 Anisotropic Heisenberg Model with a Single-Ion Anisotropy, ArXiv, no. 5, p. 2, 2006.

[66] B. Deviren, M. Keskin, and O. Canko, Magnetic properties of an anti-ferromagnetic and ferrimagnetic mixed spin-1/2 and spin-5/2 Ising model in the longitudinal magnetic field within the effective-field approximation, Phys. A Stat. Mech. its Appl., vol. 388, no. 9, pp. 1835–1848, 2009.

[67] E. Albayrak, Anisotropic Heisenberg model for the mixed spin-2 and spin-1/2 in the Oguchi approximation on the simple cubic lattice, J. Supercond. Nov. Magn., vol. 486, pp. 161–167, 2017.

[68] J. A. Reyes, N. De La Espriella, and G. M. Buendía, Effects of an external magnetic field on a mixed spin-3/2 and spin-5/2 Ising ferrimagnet: A Monte Carlo study, Phys. Status Solidi Basic Res., vol. 252, no. 10, pp. 2268–2274, 2015.

REFERENCES

[69] H. K. Mohamad, Magnetic and thermodynamic properties of a mixed spin-1and spin-7/2 Blume-Capel Ising ferrimagnetic system, Int. J. of Adv. Res., vol. 2, no. 9, pp. 442–453, 2014.

[70] L. Neel, Magnetic properties of ferrites: ferrimagnetism and antiferromagnetism, Ann. Phys, vol. 3, pp. 137–198, 1948.

LIST OF PUBLICATIONS

[1] Hasan Fareed, Hadey K. Mohamad, Spin Compensation Temperatures in the Oguchi Approximation of the Mixed Spin-3/2 and Spin-5/2 Ising Ferrimagnet, Journal of College of Education for Pure Sciences, Vol.8, No.1, pp (274-283), 2018.

الملخص

في هذا العمل البحثي تم دراسة الخواص المغناطيسية لنظام ثنائي فيريمغناطيسي خليط عزومه المغناطيسية $S_i^A = 3/2$ و $S_j^B = 5/2$ من خلال حل موديل بلوم كبل ايزنك حلا عددياً و باستخدام طريقة اوكوتشي للشبائك البلورية المكعب بسيط و المكعب متمركز الأوجه على التوالي. من الجدير بالذكر انه تم تطوير النموذج المذكور من خلال صياغة هاملتوني النظام قيد الدراسة حيث تضمن إضافة حد المجال الفعال وعلى أساسه بنيت النتائج للشبائك البلورية المشار اليها أعلاه. تتلخص طريقة اوكوتشي بأنها تتعامل مع زوج منفرد من الذرات المتجاورة كوحدة واحدة وبأفتراض ان هذا الزوج من الذرات يتفاعل مع باقي الشبيكة عن طريقة المجال الفعال.

تم تغيير التباينات البلورية المغناطيسية بدقة لغرض تفحص ظواهر جديرة بالاهتمام و هي ظاهرة التعادل المغناطيسي ودالة الطاقة الحرة للنظام المعني حيث وجدنا ان النظام المغناطيسي في ضوء موديل بلوم كبل ايزنك يمتلك درجة حرارة تعادل واحدة عندما $(D_B/|J| = -2.8)$ لشبيكة مكعب بسيط $(z = 6)$ بينما يمتلك النظام ثلاث درجات حرارية تعادلية لشبيكة مكعب بسيط (sc) عند المدى $(-1.99 \leq D_B/|J| \leq -1.85)$ و لشبيكة مكعب متمركز الأوجه (fcc) عند المدى $(-5.2 \leq D_B/|J| \leq -4.8)$. وقد لاحظنا بأن ظهور نقاط التعادل لا يعتمد على D_A/J وانما على $D_B/|J|$ فقط. بينما تؤثر $D_A/|J|$ فقط على قيمة هذه الدرجات الحرارية ولا تحدث هذه الظاهرة عند القيم الموجبة للتباينات البلورية. ومن ناحية اخرى تم الحصول على مجموعة من الاشكال المختلفة وهي Q, P, S, N, L, M Type لشبيكة المكعب البسيط (sc) و Q, S, N, R, L, M Type لشبيكة المكعب المتمركز الأوجه (fcc) .

البحوث والدراسات للمركبات ذات العزوم المغناطيسية قيد الدراسة قد تم تناولها تجريبياً مثل $Cs_2Mn^{II}[V^{II}(CN)_6]$، $CsMn^{II}[Cr^{III}(CN)_6].H_2O$ و $Mn^{II}[Mn^{IV}(CN)_6].x.H_2O$ علما ان جميع المركبات المذكورة عبارة عن مغانيط جزيئية تتبلور بهيئة شبيكة متمركزة الأوجه. ان حدوث ظاهرة التعادل هو ذا أهمية تكنولوجية كبيرة حيث عند هذه النقاط الحرجة بالذات نحتاج الى اقل مقدار ممكن من المجال المعاكس لتغيير اتجاه التمغنط عند اكمال حلقة الهسترة المغناطيسية وهكذا يمكن الحصول على حلقة هسترة ذات مساحة اقل بالتالي اقل خسارة بالطاقة.

وزارة التعليم العالي والبحث العلمي

جامعة المثنى كلية العلوم

قسم الفيزياء

دراسة الخواص المغناطيسية لسبيكة ثنائية فيري مغناطيسية تحت تأثير المجالات البلورية

رسالة مقدمة كجزء من متطلبات نيل شهادة الماجستير في علوم الفيزياء

من قبل

حسن فريد فوزي

بأشراف

أ.م.د. هادي قاسم محمد

2018